Configurational Isomers and Conformational Structures of Lycopene

Gregory A. Chass

A dissertation submitted in conformity with the requirements of the Ph.D. degree

Department of Pharmacology and Pharmacotherapy

University of Szeged

Szeged, Hungary

2001

ABSTRACT

Lycopene is an effective antioxidant *in vivo* and although it is present in its all-*trans* isomeric form in fruits and vegetables, serum and tissue samples show a predominance of various *cis*-isomers of lycopene. The present study was undertaken to investigate the molecular structure of several *cis*-isomers of lycopene using an *ab initio* molecular computations. Relative stability of selected *cis*-isomers of lycopene with respect to the all-*trans* isomer was studied. The following sequence of stability was observed.

5-*cis* > all-*trans* > 9-*cis* > 13-*cis* > 15-*cis* > 7-*cis* > 11-*cis*

The first four of these isomers had relative energies within $\pm$ 1 kcal/mol, but the fifth isomer (i.e. 15-*cis*) was within 3 kcal•mol^{-1}. However, the last two isomers were less stable than the all-*trans* isomer with more than 5 kcal•mol^{-1}. Conformational study indicated that the central conjugated part of every lycopene isomer is planar. However, the two tail ends of the molecules, each containing three single C-C bonds, avoid coplanarity. Such conformations resulted in two non-equivalent C-H bond lengths in each of the two allylic pro-chiral methylene group (>C=CH-CH_2-CH_2-CH=C<). The putative mechanism of isomerization, involving one of the prochiral CH_2 groups is proposed. The exploratory conformational study was carried out on a C_1-C_8 truncated lycopene. Likewise, the mechanistic study was conducted on a C_1-C_{10} fragment model of lycopene.

DISCLAIMER

Lycopene, the principal red pigment of tomato, was probably known for over a centruy even though it was isolated in pure form only in 1910. It took about three quarters of a century to recognize its anti-oxidant actitivity. The medical importance of Lycopene became apparent in the 1990 and its role in cardiovascular medicine is now eminently obvious.

In spite of all these developments, Lycopene's mechanism of scavenging reactive oxygen species (ROS) is not well understood. The term ROS includes everything from singlet oxygen *via* superoxide anion and hydrogen peroxide, all the way to hydroxyl radical. Yet, it remians to be seen if Lycopene can react with all of them or some selected few species of ROS.

The present dissertation will concentrate on the various isomeric forms and their numerous conformational structures of Lycopene. Since the electron density distribution of all these various structural forms are different, therefore they will have different chemical reactivity. It is not unreasonable to expect that these different chemical reactivities may well predetermine the anti-oxidant activities of Lycopene isomers and conformers.

However, as the present dissertation represents a 'progress report' on Lycopene, along the lengthy road of research, the anti-oxidant activity of Lycopene will not be discussed. The dissertation, as its title suggests, will deal with the stability of the various configurational isomers and conformational structures of Lycopene.

TABLE OF CONTENTS

LIST OF TABLES

LIST OF FIGURES

ACKNOWLEDGEMENTS

The author wishes to acknowledge the encouragement of Dr. Ladislaus L. Torday (ltordai@ucalgary.ca) during this research as well as during the preparation of this dissertation. The author is also grateful to Kenneth P. Chasse (math@velocet.ca), Graydon Hoare (graydon@pobox.com), and Velocet Communications Inc. for database management, network support, software and distributive processing development. A special thanks is also extended to Andrew M. Chasse (fixy@fixy.org) for his continuing and ongoing development of novel scripting and coding techniques indirectly bringing about a reduction in the necessary number of CPU cycles for each computations.

PUBLISHED PAPERS

1. M. A. Berg, **G. A. Chasse**, E. Deretey, A. K. Füzéry, B. M. Fung, D. Y. K. Fung,H.Henry-Riyad, A. C. Lin, M. L. Mak, A. Mantas, M. Patel, I. V. Repyakh, M. Staikova, S. J. Salpietro, T-H. Tang, J. C. Vank, A. Perczel, Ö. Farkas, L. L. Torday, Z. Székely, I. G. Csizmadia Prospects in computational molecular medicine. A millennial mega-project on peptide folding THEOCHEM 500:5-58, **2000**

   IF: **1.048**

2. **G. A. Chass**, K.P. Chasse, A. Kucsman, L. L. Torday and J. Gy. Papp, Conformational Potential Energy Surfaces of a Lycopene Model, THEOCHEM **2001** (in press)

   IF: **1.048**

3. **G. A. Chass**, M. L. Mak, E. Deretey, I. Farkas, L. L. Torday, J. Gy. Papp, D. S. R. Sarma, A. Agarwal, S. Chakravarthi, S. Agarwal, A. V. Rao An *Ab Initio*Computational Study on Selected Lycopene Isomers THEOCHEM **2001** (in press)

   IF: **1.048**

4. J. C. Yueng, **G. A. Chass**, E. J. Frondozo, L. L. Torday and J. Gy. Papp, Cationic Intermediates. An Exploratory *Ab Initio* Study of *trans→cis* Isomerization Reactions of Allylic Systems THEOCHEM **2001** (in press)

   IF: **1.048**

PUBLISHED AND ACCEPTED PAPERS :

Cummulative IF : 4.192

First Author in : 2

DECLARATION

In order to comply with the accepted tradition, the main body of this dissertation is based on the four papers either published or in press. The results of any computations which were carried out after the submission of the four papers, are summarized in the Appendices.

1. PREAMBLE

1.1 Oxidative Stress

Oxidative stress is a widely used but rather ambiguous term. Generally it refers to an imbalance in which the intracellular quantity of reactive oxygen species (ROS) increases relative to the capacity of the cell to eliminate these radical-type species. Free radicals are now known to play an important role in many areas of biology. These reactive species can be beneficial to an organism (e.g. radicals produced during phagocytosis) as well as harmful (e.g. protein and DNA damage or lipid peroxidation). Various situations, including illness, demanding physical tasks, consuming fatty meal in excess, or just aging itself generates oxidative stress and can exhaust our antioxidant reserves. It is currently widely accepted that increases in oxidative stress are involved in a variety of diseases such as diabetes[1], atherosceloris, and essential hypertension[2,3].

An estimated 2-4 % of the O_2 inhaled by organisms is reduced to species that could be highly reactive. The reduction of O_2 to what are referred to as reactive oxygen species (ROS) is summarized as follows. The one-electron reduction of O_2 produces the superoxide anion radical (O_2-•); once produced, many of these molecules are quickly dismutated by a ubiquitously distributed family of metalloenzymes, the superoxide dismutases (SOD), to generate hydrogen peroxide (H_2O_2). Since it has no unpaired electron, H_2O_2 is not a free radical *per se*. H_2O_2 is either enzymatically degraded to nontoxic products or, in the presence of a transition metal, it is converted to the highly toxic hydroxyl radical (•OH).

The most reactive radical, which is likely to arise in a biological system, is hydroxyl radical (HO•). The most often quoted source of HO• in biological systems is the reductive cleavage of H_2O_2 by a reduced metal ion which is usually Fe(II). Such a process is frequently referred to as the Fenton reaction:

$$Fe(II) + H_2O_2 \rightarrow Fe(III) + HO(-) + HO\bullet \qquad (1)$$

Thus, the presence of Fe(II) and H_2O_2 can lead to HO•; this species will indiscriminately initiate a cascade oxidative free radical reactions. The source of H_2O_2 can be formed by a direct two-electron reduction of oxygen as well as by a one-electron reduction which produces superoxide anion [$O_2(-)$] in the first step. The latter species appears to be more dangerous, because, eventually, it will not only result in the production of H_2O_2, *via* suproxide dismutase, but $O_2(-)$ can act as a reducing species, and may convert Fe(III) to Fe(II) providing all the necessary components for the Fenton reaction.

As a general rule, in free radical reactions, the hydroxyl radical almost always oxidize while suproxide anion almost always reduce any biological molecule. Besides DNA demage, probably the most harmful effect generated lipid peroxidation of poly-unsaturated fatty acids (PUFA). Their bis-allylic hydrogens (PUFA-H) are especially susceptible to peroxidation. The initiation of of lipid peroxidation is given in **(2)**.

PUFA-H + •X -> PUFA• + H-X **(2)**

Propagation of this chain reaction is both thermodynamically and kinetically favoured as the reaction proceeds smoothly with O_2 as shown in **(3)** and **(4)**.

PUFA• + O_2 -> PUFA-O-O• **(3)**

PUFA-O-O• + PUFA-O-O• -> PUFA-O-OH + PUFA• **(4)**

It can be seen that the PUFA• radical is reformed while a PUFA-H became peroxidized.

Fortunately, the small rate constant of step **(4)** permits that lipid soluble antioxidants (e.g. Vitamin E, i.e.Tocopherol or TOH for short) could overcompensate the propagation reaction as shown in **(5)**.

TOH + PUFA-O-O• -> PUFA-O-OH + TO• **(5)**

Antioxidative defense mechanisms fall into two categories, nonenzymatic (direct free radical scavengers) and enzymatic processes (during which the degradation of free radicals or their intermediates is catalyzed by specific enzymes). There are a wide variety of nonenzymatic antioxidants. Most of these are for the most part small molecules and include α-tocopherol (Vitamin E), ascorbic acid (Vitamin C), glutathione, uric acid, etc. Lycopene may also be included in this list. Their efficacies as free radical scavengers depend on their antioxidant properties and solubility in lipid or aqueous media.

Endothelium-derived nitric oxide plays an important role in the regulation of vascular tone *via* stimulation of vascular smooth muscle relaxation, and it also exhibits a number of beneficial effects on conditions associated with oxidative stress. Recently, it has also been demonstrated that nitric oxide also plays a crucial role in the central nervous system: it is involved in neuromodulation, neurotransmission and synaptic plasticity. A body of accumulating data, on the other hand, indicates that nitric oxide could act as an antioxidant as well as a prooxidant[4].

Free radicals and their metabolites have been known for their effect upon mechanisms regulating cellular function. Recently it has been demonstrated that ischaemic tissue damage can result in the release of free radicals which can further add to the deleterious consequences of the infarction cascade. Free radical scavenger drugs and antioxidants are fairly recent entrants to the list of possible therapeutic approaches for treatment of acute stroke, cardiac ischemia, intestinal ischemia and arrhythmia.

1.2 Cardiac Injury

Myocardial cellular injury associated with the reperfusion of ischemic myocardium has been attributed to many interrelated factors. One of these factors, which has not yet been rigorously explored, is free radical mechanisms. The participation of free radicals has been hypothesized from the beneficial effect of antioxidative enzymes and free radical scavengers, on myocardial function.

More recently, free radicals have been directly identified in the ischemic and reperfused heart. There is no question that free radicals are involved but their origin is unknown. Free radicals are formed in the ischemic reperfused heart; they react with

polyunsaturated fatty acid also generated during ischemia and reperfusion. However, all biological tissues are protected against free radical injury by the natural occurrence of free radical scavengers and antioxidants.

Many studies in animals were conducted to prove that, due to the deleterious effects of oxygen, the stunned myocardium may derive free radicals. In most of the studies treatment with free radical scavenging agents was initiated prior to the brief ischemic episode. Antioxidants have to provide protection to the stunned myocardium if treatment is delayed.

In theory antioxidant agents administered during occlusion or at the time of reperfusion must blunt postischemic contractile disfunction. Using the canine model several authors have reported that antioxidants and scavengers administered prior to coronary occlusion or at the time of reperfusion, protect the previously ischemic tissue from reperfusion injury.

To assess the effect of a new antioxidative agent it is suggested to conduct studies in canine models with permanent coronary artery occlusion. The dogs have to be treated prior to coronary artery embolization and post occlusion to observe the effect of the compound on the size of myocardial infartion.

It is known that oxygen-derived free radicals play a critical role in the development of life-threatening arrhythmias possibly during ischemia but more especially upon abrupt reperfusion. During early reperfusion of previously ischemic tissues the sudden influx of oxygen boosted by reactive hyperemia will in the presence of reduced metabolic intermediates accumulated during the ischemic period provide an ideal situation for the formation of free radicals. The consequences of excessive free radicals formation over and above the capacity of the tissues to protect against these damaging species include peroxidation of cell membrane lipids and enzymes damage as a result of the formation of disulfide cross-bridges. These events can lead to ionic disturbances which, if severe enough, could precipitate the development of lethal arrhythmias.

2. CHOICE OF TOPIC

Lycopene is a very powerful antioxidant. It is a long chained hydrocarbon with an internal symmetry when the molecule is in its fully extended form. The symmetry element is a C_2 rotational axis oriented perpendicular to the plane of the molecule. Lycopene is an unsaturated hydrocarbon; it contains 13 double bonds. One of these double bonds is located at the center of the molecule, where the C_2 axis is passing through at the mid-point of this double bond. Six additional double bonds are located within each of the two sides. Thus, the molecule is capable to exhibit cis/trans isomerization, involving all non-symmetrically substituted double bonds. Also, each sides of the molecule possess a saturated moiety of $-CH_2-CH_2-$. Consequently, the molecule may have a variety of conformers of different stability. These conformers are associated with the rotation about the three single bonds of the dimethylene moiety connected to the olefinic units, $=CH-CH_2-CH_2-CH=$, which occurs at both sides of lycopene. It may further be recognized that the above pair of CH_2 groups contains allylic hydrogens, which are rather reactive and could thereforebe involved in the *trans* → *cis* isomerization process.

All of these features made the lycopene molecule to be very attractive choice of research topic

3. INTRODUCTION

3.1 Biological Background

Several chronic diseases, amongst which are cancer and cardiovascular diseases, are related to oxidative stress which is now recognized as an important etiological factor. Antioxidants are effective in reducing the damaging effect of oxygen containing radicals and radicaloids such as •OH, O_2^-, H_2O_2 as well as that of singlet oxygen $^1O_2$. Lycopene is a carotenoid type antioxidant, present in tomatoes and other fruits and vegetables. Studies have shown that lycopene acts as an antioxidant *in vivo*, providing protection against the oxidation of lipids, proteins and DNA [5,6]. A recently published review[7] indicated a significant inverse correlation between the intake and therefore the serum concentrations of lycopene and the risk of several diseases including cancer. In the absorption and bio-availability the isomeric forms of lycopene appear to play an important role.

3.2 Structural Background

The skeleton of lycopene [$C_{40}H_{56}$] consists of eight isoprenic units, thus it is related to tetraterpenes [$C_{40}H_{64}$] even though it contains fewer hydrogens and therefore more double bonds. Its composition is shown in **I** in its fully extended form which is the all *trans*-lycopene. As such, lycopene is closely related to β-carotenes.

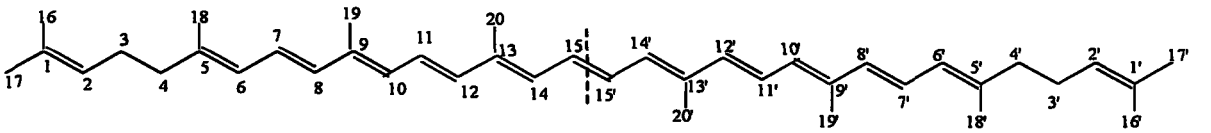

I

There are times when the structure of lycopene is presented in a pre-folded form (**II**) to show its structural similarity to β-carotene. Due to the internal molecular symmetry, it has been traditional to number the chain from the two ends as shown in **I** and **II**.

The history of lycopene[8–15] reveals an interesting story from the initial curiosity of a

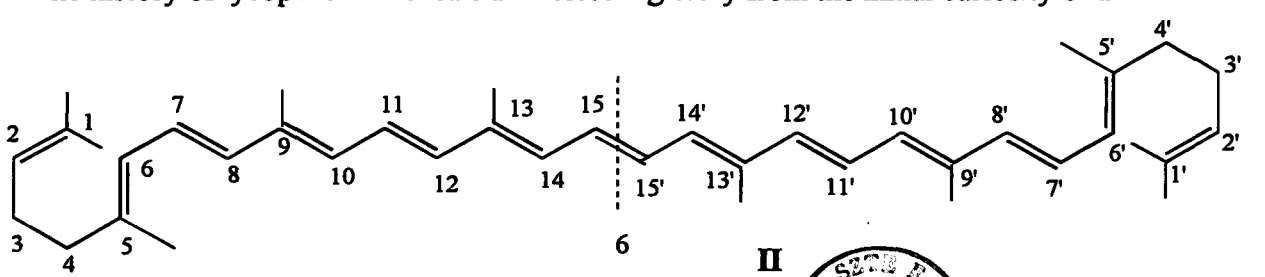

II

colourful substance in the 1910s to the medical application[5-7] in the 1990s as an antioxidant.

In 1943, Pauling pointed out [15] not all *cis*-isomers may be of equal stability due to a number of possible 1,4 interactions as shown by the following structures.

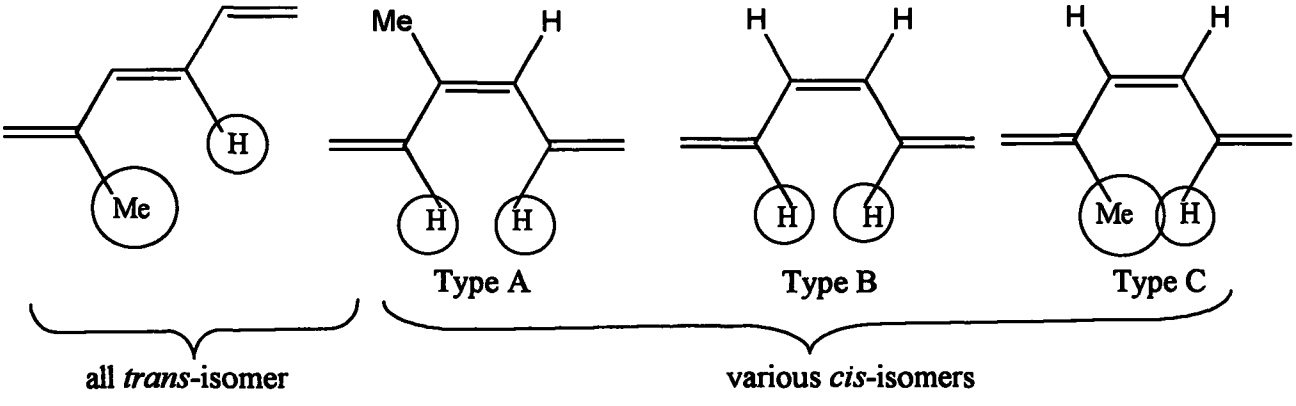

Scheme 1

Clearly, on the basis of relative group sizes, the $-CH_3$---H- interaction (type C) appears to be the most destabilizing.

No X-ray structure of lycopene has been determined as yet, however there are two X-ray structures of β-carotene in the literature.[16]

3.3 Stability Background

In fruits and vegetables Lycopene is present mostly in its all-*trans* isomeric form. However, *cis*-isomers constitute the predominant form present in the serum and tissues[13,14]. This observation suggests that at least some of the *cis*-isomers may be energetically comparable to the stability of the all-*trans* isomers. **Figure 1** shows the all-*trans*- and selected *cis*-isomers of lycopene. The relative energies for the four types of structures, depicted in **Figure 1**, are expected to exhibit four categories of stability. Consequently, we may anticipate four energy ranges as summarized in **Table 1**. Note that in addition to the three types (A, B, C) reported by Pauling[15] (**Scheme 1**), a fourth type (A') of interaction is also noted here.

Type A' is very similar to *Type A* (see **Figure 1**) except that the hydrogens, involved in 1,4 interactions (attached to carbons 4 and 7), are not eclipsed but staggered. This is illustrated in greater detail in **Table 1** and **Scheme 2**.

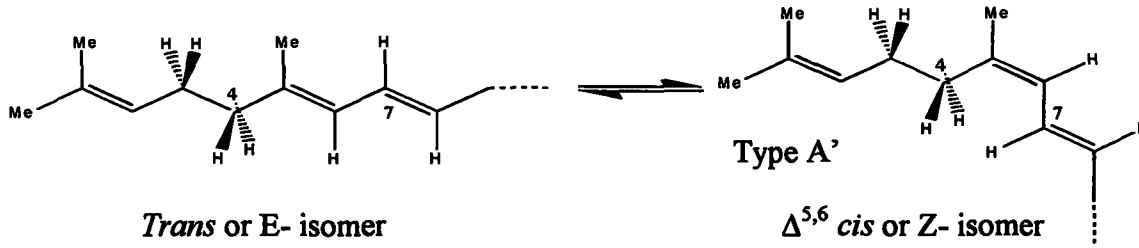

Scheme 2

Table 1 - Classification of various *cis*-lycopene isomers according to 1,4-non-bonded interactions and extent of substitution about the carbon-carbon double bond involved.

1,4-non bonded interaction		Isomers	Isomerisation with different degree of substitution
Type	*cis* structure		
A'	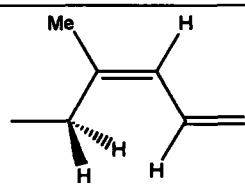	5-*cis*	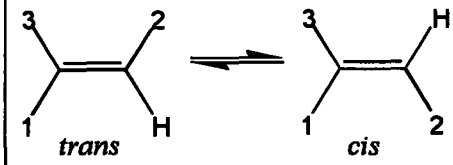
A	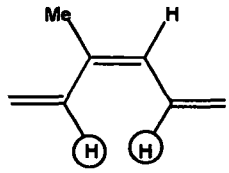	9-*cis* and 13-*cis*	
B	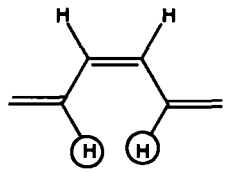	15-*cis*	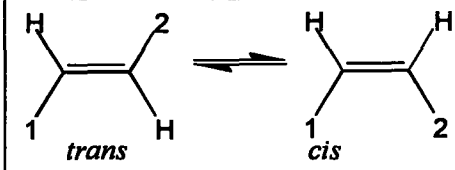
C	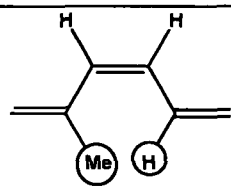	7-*cis* and 11-*cis*	

NB: Clearly, on the basis of relative group sizes , the $-CH_3$—H- interaction (type C) appears to be the most destabilizing. The order of expected stability is the following: A'>A>B>C.

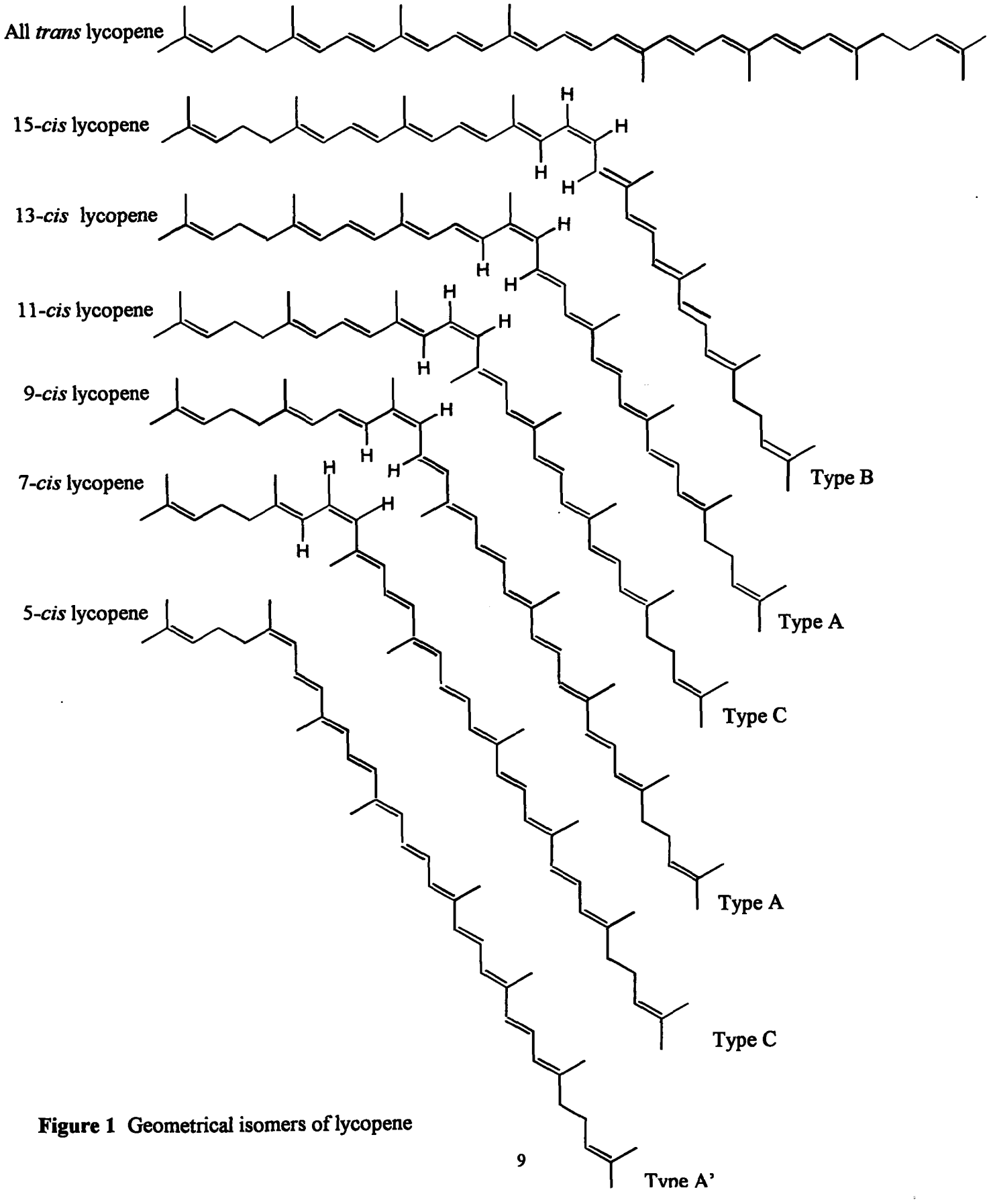

Figure 1 Geometrical isomers of lycopene

4. AIM OF STUDY

The presence of three consecutive carbon-carbon single bonds (C^2-C^3-C^4-C^5) suggests conformational flexibility of the tail-ends of lycopene. It has been deemed desirable, therefore to study the conformational intricacy of the tail-end of lycopene by choosing some model compound. If one looks at the lycopene structure, one can cut out from the full molecule shorter segments and terminate them with hydrogen atoms. These model compounds are labelled in **Scheme 3** as **Model A, Model B, Model C, Model D,** etc.

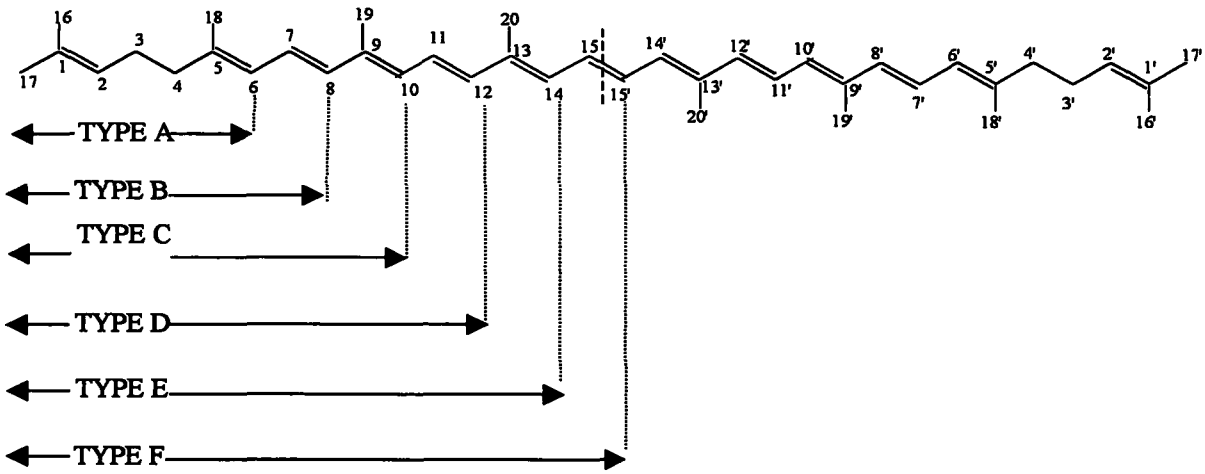

Scheme 3

For the present study we have chosen both **Model B** and **Model C,** as well as the full lycopene structure. **Model B** was used to mimic conformationally the tail-end of the all-*trans* isomer, as well as the 5-*cis* isomer. **Model C** was used to mimic the isomerization mechanism converting the all-*trans* isomer to the 5-*cis* and 7-*cis* isomers. The full lycopene was used to determine the relative stabilities of the all all-*trans* and the six *cis*-isomers.

5. METHOD

The all-*trans*- and the selected six *cis*-isomers (*5*-, *7*-, *9*-, *11*-, *13*- and *15*-) had to be explored computationally in their molecular entirety (containing 296 electrons and 96 atoms, which corresponds to 282 geometrical parameters to be optimized). Thus, lycopene may well be among the largest organic molecules investigated, using *ab initio* molecular computation, with the current computational technology. The two truncated lycopene models : **Model B** (C^1-C^8 segment) and **Model C** (C^1-C^{10} segment) are shown below in **Scheme 4**.

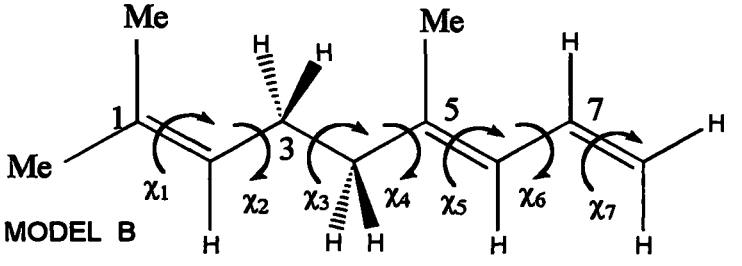

X_1: Me-C_1-C_2-C_3
X_2: C_1-C_2-C_3-C_4
X_3: C_2-C_3-C_4-C_5
X_4: C_3-C_4-C_5-C_6
X_5: C_4-C_5-C_6-C_7
X_6: C_5-C_6-C_7-C_8
X_7: C_6-C_7-C_8-H

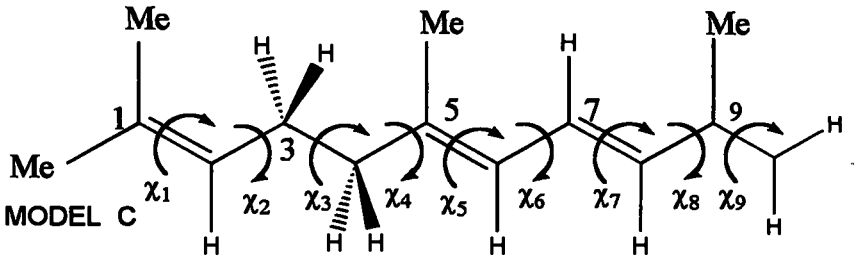

X_1: Me-C_1-C_2-C_3
X_2: C_1-C_2-C_3-C_4
X_3: C_2-C_3-C_4-C_5
X_4: C_3-C_4-C_5-C_6
X_5: C_4-C_5-C_6-C_7
X_6: C_5-C_6-C_7-C_8
X_7: C_6-C_7-C_8-C_9
X_8: C_7-C_8-C_9-C_{10}
X_9: C_8-C_9-C_{10}-H

Scheme 4

The conformational PEHS, as specified by equation **(6)**, illustrated schematically in **Figure 2**, is applicable for both **Model B** and **Model C**.

$$E=f(\chi_2, \chi_3, \chi_4) \qquad (6)$$

Standard geometry optimizations were performed on the all-*trans* as well as six selected *cis*-isomers of the full lycopene molecule. The computations were carried out using the Gaussian 98 program system.[17] Every structure was computed first at the RHF/3-21G level of theory. Subsequently, geometry optimizations were carried out on

selected structures at the RHF/6-31G(d, p) and B3LYP/6-31G(d, p) levels of theory. The results of the higher level computations are reported in the Appendix.

6. RESULTS AND DISCUSSION

6.1 Molecular Structure of Lycopene Model B

When a planar moiety is rotated about a tetrahedral carbon, it may be either eclipsed with a tetrahedral bond or perpendicular to that bond. This has been revealed by the study on ethyl benzene[18]. These idealized conformers as applied for lycopene **Model B** are illustrated by **Scheme5**.

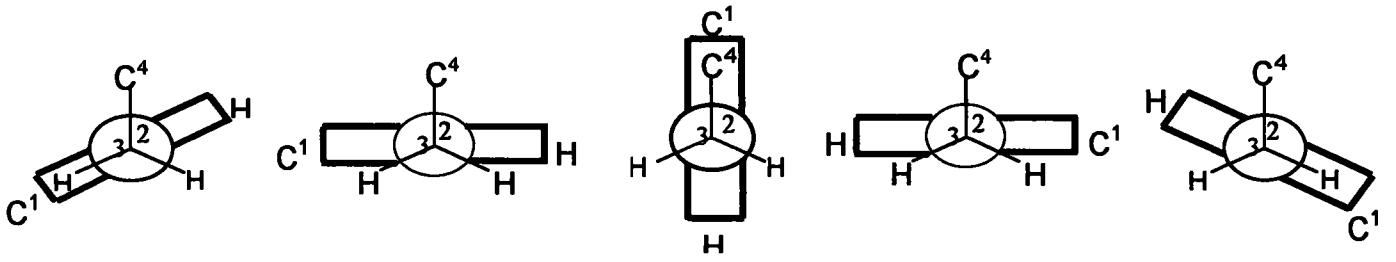

χ^1 =-120° χ^1 = -90° χ^1 = 0° χ^1 = 90° χ^1 = 120°

Scheme 5

Single scans can be carried out to study the rotation about the C^2-C^3(χ_2), C^3-C^4(χ_3) and C^4-C^5(χ_4) single bonds of **Model B**. However, the conformational problem is better studied in the form of a potential energy hyper-surface (PEHS), which involves all three torsional angles **(6)**.

The rotation (see **Scheme 4**) about the single C^3-C^4 bond (χ_3) is expected to be in g^+, *a*, g^- configurations, therefore three potential energy surfaces (PES) may be generated at these three orientations of χ_3.

$$E=f(\chi_2, \chi_4) \quad \text{at} \quad \chi_3=+60° \qquad (7a)$$

$$E=f(\chi_2, \chi_4) \quad \text{at} \quad \chi_3=+180° \qquad (7b)$$

$$E=f(\chi_2, \chi_4) \quad \text{at} \quad \chi_3=+300°(-60°) \qquad (7c)$$

These 2D cross-sections are shown as three levels in **Figure 2.**

One may also generate 1D cross-sections such as :

$$\mathbf{E=f(\chi_2)} \quad \textbf{at} \quad \chi_3=180° \quad \chi_4=\pm 90° \qquad \textbf{(8a)}$$

$$\mathbf{E=f(\chi_3)} \quad \textbf{at} \quad \chi_2=\pm 90° \quad \chi_4=\pm 90° \qquad \textbf{(8b)}$$

$$\mathbf{E=f(\chi_4)} \quad \textbf{at} \quad \chi_2=\pm 90° \quad \chi_3=180° \qquad \textbf{(8c)}$$

The location of these conformational potential energy curves (PEC) are indicated by three heavy solid lines and three heavy broken lines in **Figure 2.** The two sets of the three cross-sections are equivalent.

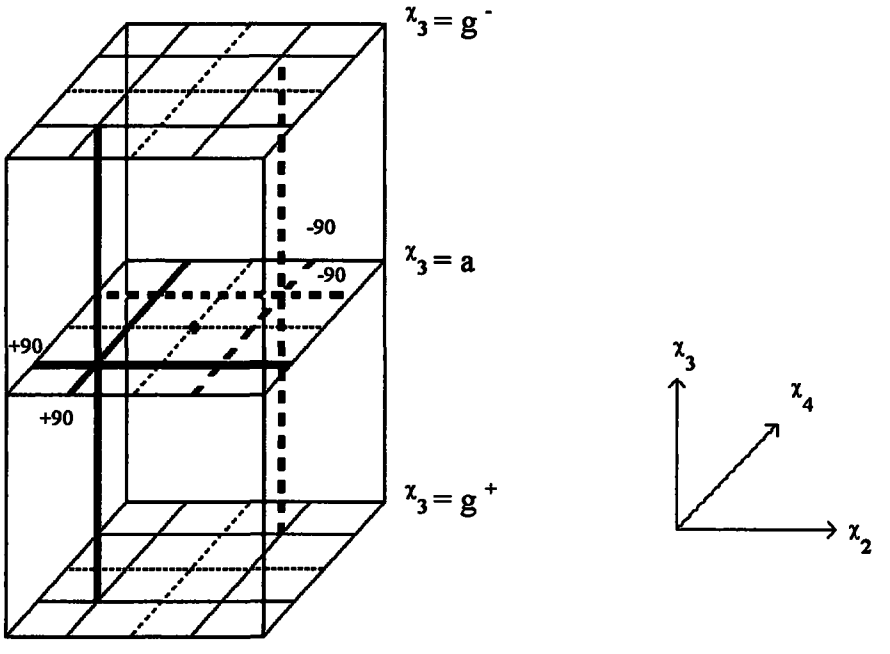

Figure 2 A schematic representation of the conformational PEHS, $E=f(\chi_2, \chi_3, \chi_4)$ of lycopene **Model B**. The heavy dot, at the centre, illustrates the location of the fully symmetric conformation as drawn in **III**. The three levels indicate the three 2D cross-sections (PES) and the three perpendicular heavy broken and solid lines specify the locations of the three 1D cross-sections (PEC) investigated.

Perhaps it should be emphasized that the conformational PEHS, as specified by equation (1), illustrated schematically in **Figure 2**, is applicable for both the all-*trans* and for the 5-*cis*-isomer of lycopene **Model B**.

6.1.1 The All-trans-Structure of Lycopene Model B

The all-*trans*-lycopene **Model B** was subjected first to conformational analysis. The conformational PEHS **(6)** of three independent variables, was investigated in terms of three PESs **(7)** of two independent variables. These three PESs are depicted in landscape and contour representations in **Figure 3.** In the central part of **Figure 3**, χ_3 was kept in its *anti*-position **(7b)**. At the lower part of **Figure 3**, χ_3 was kept in *g*+ **(7a)** and for the top portion of **Figure 3**, χ_3 was kept in *g*- **(7c)** position. Clearly, the central level of **Figure 2**, for which the PES **(7b)** is depicted in the center of **Figure 3**, is the most symmetric. By inspection, we may anticipate the presence of nine minima on the PES. These are listed in **Scheme 6**.

[s(a)s]	**[*g*+(a)s]**	**[*g*-(a)s]**	**[s(a)s]**
s(a)*g*-	***g*+(a)*g*-**	***g*-(a)*g*-**	**[s(a)*g*-]**
s(a)*g*+	***g*+(a)*g*+**	***g*-(a)*g*+**	**[s(a)*g*+]**
s(a)s	***g*+(a)s**	***g*-(a)s**	**[s(a)s]**

Scheme 6

Those minima located at the edges are repeated twice and the structure at the corner is repeated four times. These repeated structures are shown in square brackets, leaving nine unique conformers (which are not in square brackets). Since there are three levels, as shown in **Figure 2**, the three PESs (**Figure 3**) may contain up to 3x9 = 27 stable conformations. The 1D scans leading to the three PECs (shown at the left hand side of **Figure 4**) indeed suggest the existence of three unique minima, on each of the three PECs. This reconfirms that $3^3 = 27$ minima may be anticipated. However, sometimes expected minima are annihilated from the PES[19]. Nevertheless, geometry optimizations have been initiated on these 27 conformations.

The optimized torsional angles are summarized in **Table 2**. Indeed a few minima, involving some *syn* orientations, were annihilated. In this table, the torsions about the single bonds (χ_2, χ_3 and χ_4) are shown in bold. Other torsional angles (χ_5, χ_6 and χ_7) are associated with double bonds. Since this is the all-*trans* form, these double bonds should have dihedral angles in the vicinity of ±180°. However, the last double bond is ending in CH_2, so one of the two hydrogens is *trans* (χ_7) and the other is *cis*. In **Table 2**, the last three dihedral angles (χ_8, χ_9 and χ_{10}) measure the spatial orientations of the three methyl groups of **Model B**.

The four central minima, shown in **Scheme 6**, represent the two most stable conformations. They are pairwise equivalent but they all practically have the same stability as shown in terms of ΔE (kcal•mol^{-1}), in **Scheme 7**. The relative energies, together with the computed dipole moments, are summarized in **Table 3**.

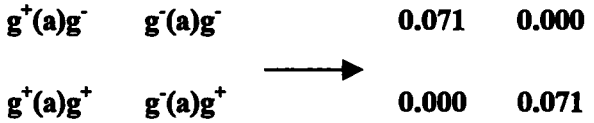

Scheme 7

In addition to the nine structures in **Scheme 6**, where the central letter in parentheses represents *anti* orientation, (*a*), along χ_3, there are two additional sets of 9 structures; one set with (*g*+) and the other with (*g*-).

It is interesting to compare the top and bottom surfaces of **Figure 3**. They are centrosymmetric to each other through the fully symmetric (*a, a, a*) focal point, denoted as a heavy dot in **Figure 2**. For this reason, the two sides of the 1D cross-section (**8b**), corresponding to the central left hand side PEC, in **Figure 4**, along with the heavy vertical line in **Figure 2**, are not completely symmetrical. The *g*+ and *g*- minima differ slightly because the two surfaces at $\chi_2 = \chi_4 = 90°$, are not identical.

The centrosymmetric arrangement can also be seen from the relative energies in **Scheme 8**.

0.338	0.796	$g^+(g^+)g^-$	$g^-(g^+)g^-$	$g^+(g^-)g^-$	$g^-(g^-)g^-$	1.062	1.302
1.301	1.063	$g^+(g^+)g^+$	$g^-(g^+)g^+$	$g^+(g^-)g^+$	$g^-(g^-)g^+$	0.796	0.338

Scheme 8

The discrepancies (1.063 versus 1.062 and 1.301 versus 1.302) are the result of regular optimization, which are expected to disappear when the optimizations are performed to a tight convergence threshold.

6.1.2 The 5-cis-structure of Lycopene Model B

The conformational PEHS **(6)** of three independent variables, shown schematically in **Figure 2** for the all-*trans*-isomer, is also valid for the 5-*cis*-isomer. In the case of the 5-*cis*-isomer, just as before, three PESs of two independent variables were generated for the $\chi_3 = g^+$ a, and g^- orientations. These are shown in **Figure 5** as bottom central and top surfaces, respectively. The 1D-scans produced three PECs (shown at the right hand side of **Figure 4**).

The centrosymmetric arrangement can be seen from the relative energies, analogously to the all-*trans*-form, in the case for $\chi_3 = anti$, in **Scheme 9**.

$g^+(a)g^-$	$g^-(a)g^-$	-0.157	-0.314
$g^+(a)g^+$	$g^-(a)g^+$	-0.314	-0.157

Scheme 9

Similarly, the centrosymmetric character of the PEHS can be further demonstrated by comparing the relative energies for the $\chi_3 = g^+$ and $\chi_3 = g^-$ cases. This is illustrated by **Scheme 10**.

0.140	0.796	$g^+(g^+)g^-$	$g^-(g^+)g^-$	$g^+(g^-)g^-$	$g^-(g^-)g^-$	0.518	0.795
0.795	0.518	$g^+(g^+)g^+$	$g^-(g^+)g^+$	$g^+(g^-)g^+$	$g^-(g^-)g^+$	0.804	0.140

Scheme 10

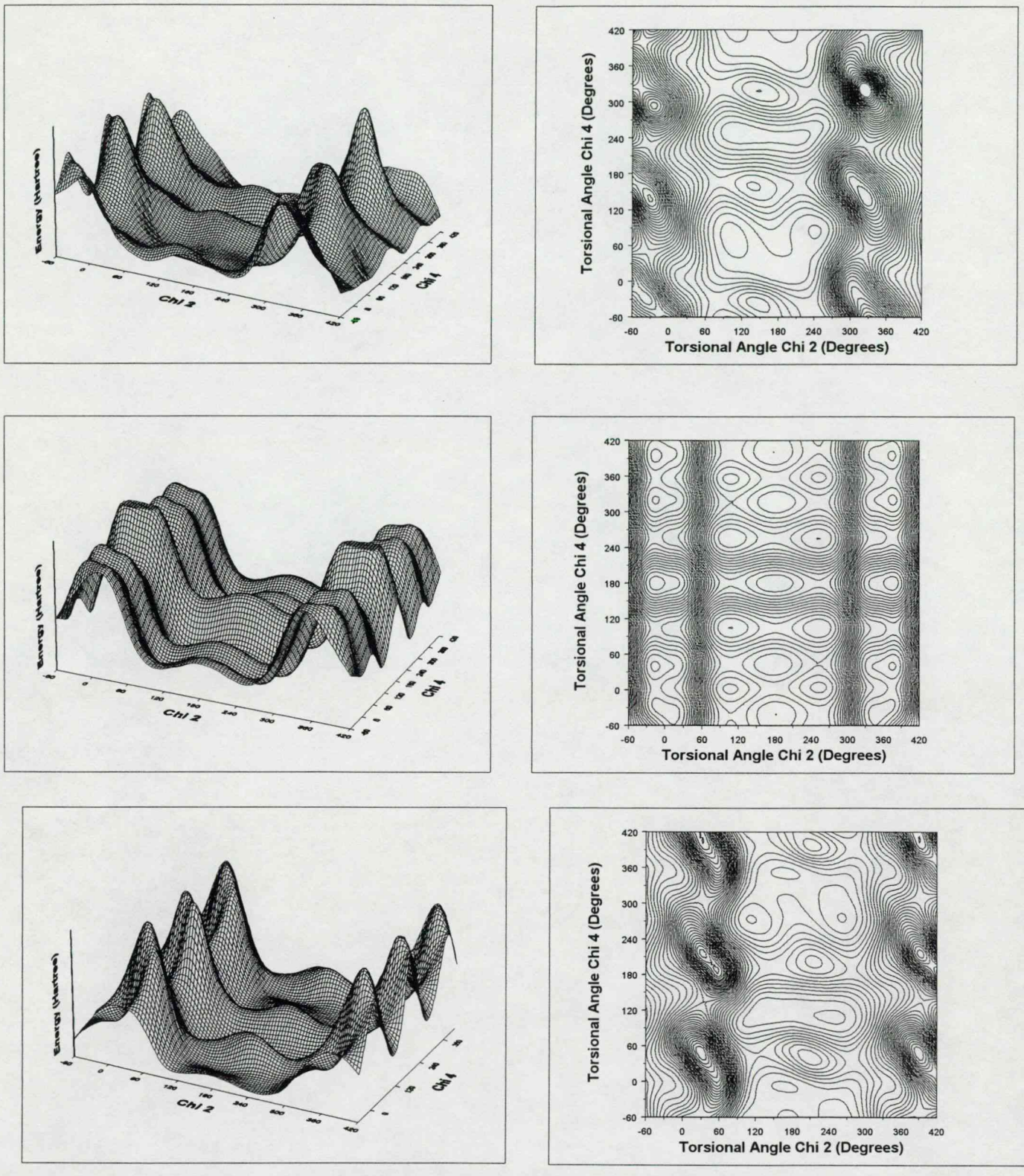

Figure 3 All-*trans*-lycopene Model B PES, E=$f(\chi_2, \chi_4)$ **Left :** Landscape representation **Right :** Contour Representation **Bottom :** at $\chi_3 = g^+$ position **Center :** at $\chi_3 =$ *anti* position **Top :** at $\chi_3 = g^-$ position

All-*trans*-Lycopene Model B

5-*cis*-Lycopene Model B

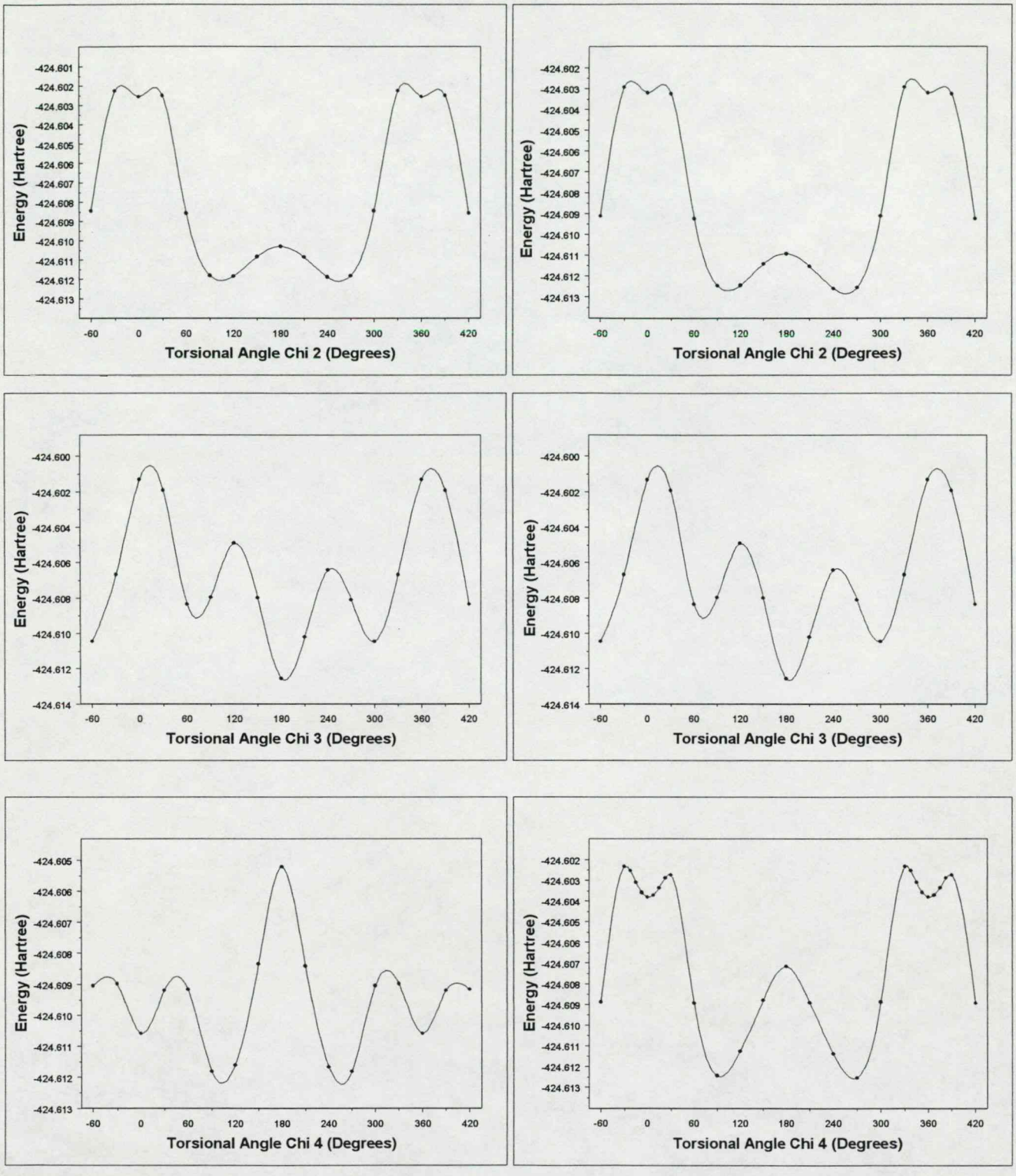

Figure 4 Conformational PECs of lycopene tail-end Model B E=$f(\chi_2)$, E=$f(\chi_3)$, E=$f(\chi_4)$, according to equation **(8a)**, **(8b)** and **(8c)**, respectively. Left-Hand side : all-*trans*-isomers. Right-Hand Side : 5-*cis*-isomers.

Table 2 - Torsional Angles of the Optimized All-*Trans* Lycopene Model B Conformers

Conformer			χ_1	χ_2	χ_3	χ_4	χ_5	χ_6	χ_7	χ_8	χ_9	χ_{10}
χ_2	χ_3	χ_4										
s	g^+	s	175.825	**8.219**	**73.456**	**-2.696**	178.530	179.109	179.882	-1.567	155.285	179.822
s	g^+	g^+			**NOT**	**FOUND**		GOES	TO	g+g+g+		
s	g^+	g-			**NOT**	**FOUND**		GOES	TO	g+g+g-		
g^+	g^+	s	-179.380	**132.366**	**70.240**	**13.795**	178.533	-179.920	-179.996	0.201	178.837	-174.271
g^+	g^+	g^+	-179.970	**99.689**	**59.014**	**79.958**	-179.141	-179.887	179.995	0.247	179.439	172.338
g^+	g^+	g-	-179.416	**117.884**	**66.164**	**-106.597**	179.837	-179.798	179.991	0.358	179.405	179.754
g-	g^+	s	-179.216	**-167.031**	**68.838**	**-0.291**	179.071	179.299	179.919	-0.315	-179.499	179.779
g-	g^+	g^+	-178.556	**-114.775**	**69.896**	**84.896**	-178.860	-179.819	-179.979	0.441	-174.256	-176.966
g-	g^+	g-	178.865	**-105.966**	**74.625**	**-98.969**	179.045	-179.44	-179.990	0.277	176.476	-173.688
s	a	s	179.961	**-1.072**	**-179.307**	**-0.550**	-179.961	179.983	179.999	0.016	179.745	179.679
s	a	g^+			**NOT**	**FOUND**		GOES	TO	g+ag+		
s	a	g-			**NOT**	**FOUND**		GOES	TO	g-ag-		
g^+	a	s	-179.165	**103.795**	**177.115**	**0.315**	179.902	179.969	-179.998	-0.037	179.214	-179.858
g^+	a	g^+	-178.935	**106.356**	**176.434**	**100.248**	-178.637	-179.798	-179.961	0.069	179.791	176.165
g^+	a	g-	-178.912	**104.305**	**177.254**	**-101.338**	178.588	179.917	179.951	0.018	179.623	-178.267
g-	a	s	179.149	**-103.829**	**-177.185**	**-0.257**	-179.901	-179.962	179.999	0.083	-179.226	179.863
g-	a	g^+	178.912	**-104.659**	**-177.163**	**101.431**	-178.588	-179.911	-179.959	0.006	-179.656	178.335
g-	a	g-	178.956	**-106.474**	**-176.451**	**-100.297**	178.637	179.818	179.963	-0.067	-179.716	-176.232
s	g-	s	-175.870	**-8.143**	**-73.563**	**2.816**	-178.526	-179.097	-179.884	1.777	155.308	-179.569
s	g-	g^+			**NOT**	**FOUND**		GOES	TO	g-g-g+		
s	g-	g-			**NOT**	**FOUND**		GOES	TO	g+g-g-		
g^+	g-	s	179.087	**167.376**	**-68.605**	**-0.093**	-179.019	-179.472	-179.921	0.683	179.219	-179.966
g^+	g-	g^+	-178.860	**105.930**	**-74.655**	**98.949**	-179.034	179.429	179.990	-0.234	183.711	173.668
g^+	g-	g-	178.624	**114.557**	**-69.915**	**-84.922**	178.840	179.807	179.986	-0.341	174.794	-176.874
g-	g-	s	179.388	**-131.690**	**-70.369**	**-13.840**	-178.554	179.922	-179.997	-0.460	-179.229	174.221
g-	g-	g^+	179.402	**-117.654**	**-66.185**	**106.482**	-179.849	179.865	-179.996	-0.269	-179.384	179.818
g-	g-	g-	179.999	**-99.757**	**-58.865**	**-79.906**	179.135	179.874	-179.997	-0.381	-179.470	-172.162

Table 3 - Dipole Moments, Total Energies and Relative Energies of the Optimized All-*Trans* Lycopene Model B Conformers

Conformer			Dipole	Energy (Hartree)	ΔEnergy (kcal•mol^{-1})
χ_2	χ_3	χ_4			
s	g^+	s	0.7430	-424.6006056	7.381
s	g^+	g^+	NOT FOUND	GOES TO g+g+g+	N/A
s	g^+	g-	NOT FOUND	GOES TO g+g+g-	N/A
g^+	g^+	s	0.8374	-424.6089342	2.155
g^+	g^+	g^+	1.0844	-424.6102939	1.301
g^+	g^+	g-	0.6797	-424.6118287	0.338
g-	g^+	s	0.6463	-424.6093099	1.919
g-	g^+	g^+	0.8069	-424.6106742	1.063
g-	g^+	g-	0.5608	-424.6110997	0.796
s	a	s	0.8259	-424.604468	4.957
s	a	g^+	NOT FOUND	GOES TO g+ag+	N/A
s	a	g-	NOT FOUND	GOES TO g-ag-	N/A
g^+	a	s	0.8872	-424.6108053	0.981
g^+	a	g^+	**0.6568**	**-424.6123678**	**0.000**
g^+	*a*	*g-*	*0.9860*	*-424.6122554*	*0.071*
g-	a	s	0.8869	-424.6108055	0.980
g-	*a*	*g^+*	*0.9861*	*-424.6122554*	*0.071*
g-	a	g-	**0.6571**	**-424.6123677**	**0.000**
s	g-	s	0.7423	-424.6006059	7.381
s	g-	g^+	NOT FOUND	GOES TO g-g-g+	N/A
s	g-	g-	NOT FOUND	GOES TO g+g-g-	N/A
g^+	g-	s	0.6492	-424.6093103	1.919
g^+	g-	g^+	0.5602	-424.6110997	0.796
g^+	g-	g-	0.8070	-424.6106747	1.062
g-	g-	s	0.8412	-424.6089341	2.155
g-	g-	g^+	0.6794	-424.6118286	0.338
g-	g-	g-	1.0843	-424.6102937	1.302

The optimized torsional angles are summarized in **Table 4** and the computed properties are given in **Table 5**.

6.1.3 Molecular configurations of Lycopene Model B

It is of considerable interest to optimize the fully symmetrical a,a,a ($\chi_2 = \chi_3 = \chi_4 = 180°$) conformation. This is done for both the all-*trans* and the 5-*cis* structures in two steps. First, these three dihedral angles were kept frozen and then subsequently relaxed. In addition to the optimized torsional angles (**Table 6**), the energies and the imaginary frequencies (**Table 7**) were also tabulated. These fully symmetric points (marked as a solid dot at the centre of **Figure 2**) are second order saddle points. All these indicate that neither the all-*trans* nor the 5-*cis* isomers, are ever fully symmetric. Consequently, neither the all-*trans* nor the 5-*cis* isomers are planar.

It is interesting to compare the relative stability of the all-*trans*- and the 5-*cis*-isomers. Intuitively, one would have guessed that all 5-*cis*-conformers have to be of higher energy than their corresponding all-*trans*-conformers. This is not the case here however, as may be seen from of the relative energies given in **Table 3** and **5**, is shown in **Figure 10.**

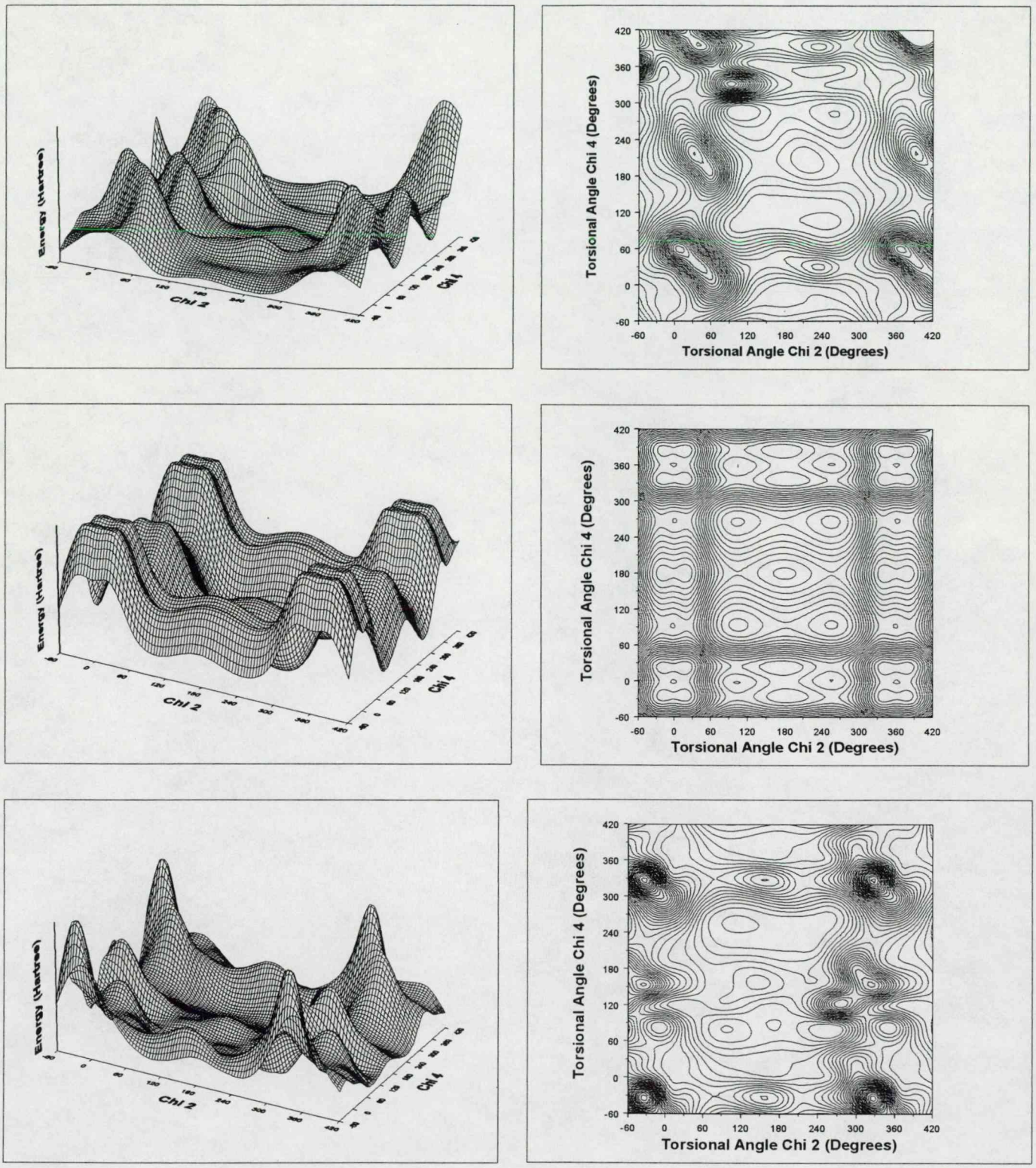

Figure 5 The 5-*cis*-lycopene Model B PES, E=$f(\chi_2, \chi_4)$ **Left :** Landscape representation **Right :** Contour Representation **Bottom :** at $\chi_3 = g^+$ position **Center :** at $\chi_3 =$ *anti* position **Top :** at $\chi_3 = g^-$ position

Table 4 - Torsional Angles of the Optimized 5-*Cis* Lycopene Model B Conformers

Conformer			χ_1	χ_2	χ_3	χ_4	χ_5	χ_6	χ_7	χ_8	χ_9	χ_{10}
χ_2	χ_3	χ_4										
s	g^+	s	176.805	**-9.080**	**88.036**	**-8.820**	-4.471	170.478	-181.311	-1.685	163.845	178.980
s	g^+	g^+			**NOT**	**FOUND**		GOES	TO	sg+s		
s	g^+	g-			**NOT**	**FOUND**		GOES	TO	g-ag-		
g^+	g^+	s	-179.548	**170.359**	**67.397**	**8.997**	-3.028	170.953	179.136	-0.132	179.930	-177.086
g^+	g^+	g^+	-179.959	**99.783**	**58.797**	**79.371**	1.400	-177.716	-179.580	0.255	179.460	175.630
g^+	g^+	g-	-179.283	**115.906**	**67.994**	**-101.947**	0.596	-178.190	-179.796	1.003	179.588	-178.130
g-	g^+	s			**NOT**	**FOUND**		GOES	TO	g-ag-		
g-	g^+	g^+	-178.880	**-112.982**	**68.508**	**80.618**	0.963	-177.246	-179.686	0.296	-174.921	178.317
g-	g^+	g-	178.111	**-105.361**	**75.434**	**-100.127**	-0.038	-178.714	179.961	-2.349	177.781	-177.214
s	a	s			**NOT**	**FOUND**		GOES	TO	g+ag+		
s	a	g^+			**NOT**	**FOUND**		GOES	TO	g+ag+		
s	a	g-			**NOT**	**FOUND**		GOES	TO	g+ag+		
g^+	a	s	-179.140	**102.780**	**174.547**	**4.853**	0.122	-179.743	-179.872	-0.077	179.099	-178.543
g^+	a	g^+	-178.901	**104.375**	**175.566**	**91.422**	1.315	-178.676	-179.966	-0.001	179.400	176.023
g^+	a	g-	-178.948	**103.802**	**179.675**	**-91.919**	-1.255	179.048	179.795	0.009	179.441	-176.171
g-	a	s	179.155	**-102.865**	**-174.684**	**-4.575**	-0.114	179.658	179.875	0.129	-178.869	178.668
g-	a	g^+	178.939	**-103.962**	**-179.632**	**91.951**	1.255	180.915	-179.994	0.014	-179.392	176.131
g-	a	g-	178.916	**-104.231**	**-175.582**	**-91.459**	-1.320	178.750	179.970	-0.021	-179.484	-175.989
s	g-	s	-176.782	**9.068**	**-88.104**	**8.891**	4.444	-170.539	-178.691	1.637	-163.802	-178.947
s	g-	g^+			**NOT**	**FOUND**		GOES	TO	g-g-g+		
s	g-	g-			**NOT**	**FOUND**		GOES	TO	g-g-g-		
g^+	g-	s			**NOT**	**FOUND**		GOES	TO	g-g-g+		
g^+	g-	g^+	-178.115	**105.325**	**-75.373**	**100.166**	0.061	178.649	-179.960	-2.389	-178.038	176.975
g^+	g-	g-	178.875	**113.110**	**-68.478**	**-80.610**	-0.968	177.325	179.680	-0.360	174.822	-178.339
g-	g-	S	179.535	**-170.224**	**-67.490**	**-8.822**	3.006	-171.005	-179.135	0.295	-179.345	177.220
g-	g-	g^+	179.289	**-115.815**	**-68.005**	**101.908**	-0.598	178.149	179.799	-0.988	-179.589	178.083
g-	g-	g-	179.946	**-99.765**	**-58.836**	**-79.395**	-1.406	177.812	179.582	-0.159	-179.349	-175.527

Table 5 - Dipole Moments, Total Energies and Relative Energies of the Optimized 5-*Cis* Lycopene Model B Conformers

Conformer			Dipole	Energy (Hartree)	ΔEnergy (kcal•mol^{-1})
χ_2	χ_3	χ_4			
s	g^+	s	0.8089	-424.5945699	11.168
s	g^+	g^+	NOT FOUND	GOES TO sg+s	N/A
s	g^+	g-	NOT FOUND	GOES TO g-ag-	N/A
g^+	g^+	s	0.8657	-424.6023298	6.299
g^+	g^+	g^+	1.0293	-424.6111013	0.795
g^+	g^+	g-	0.7313	-424.6121441	0.140
g-	g^+	s	NOT FOUND	GOES TO g+ag+	N/A
g-	g^+	g^+	0.7078	-424.6115428	0.518
g-	g^+	g-	0.5608	-424.6110997	0.796
s	a	s	NOT FOUND	GOES TO g+ag+	N/A
s	a	g^+	NOT FOUND	GOES TO g+ag+	N/A
s	a	g-	NOT FOUND	GOES TO g-g-g+	N/A
g^+	a	s	0.9719	-424.6040333	5.230
g^+	a	g^+	**0.6513**	**-424.6128689**	**-0.314**
g^+	a	g-	**0.9975**	**-424.6126178**	**-0.157**
g-	a	s	0.9716	-424.6040331	5.230
g-	a	g^+	**0.9976**	**-424.6126178**	**-0.157**
g-	a	g-	**0.6515**	**-424.6128689**	**-0.314**
s	g-	s	0.8091	-424.5945699	11.168
s	g-	g^+	NOT FOUND	GOES TO g-g-g+	N/A
s	g-	g-	NOT FOUND	GOES TO g-g-g-	N/A
g^+	g-	s	NOT FOUND	GOES TO g-g-g+	N/A
g^+	g-	g^+	0.6145	-424.6110874	0.804
g^+	g-	g-	0.7079	-424.6115427	0.518
g-	g-	s	0.8654	-424.6023291	6.299
g-	g-	g^+	0.7314	-424.6121441	0.140
g-	g-	g-	1.0296	-424.6111013	0.795

Table 6 - Torsional Angles of the Symmetric 2nd Order TS of Lycopene Model B Isomers

Conformer	χ_1	χ_2	χ_3	χ_4	χ_5	χ_6	χ_7	χ_8	χ_9	χ_{10}
Trans	179.973	180.000	180.000	180.000	180.000	179.996	180.000	0.181	180.124	180.121
5-*Cis*	180.001	180.000	180.000	180.000	-0.0008	180.001	-179.999	0.025	180.005	179.981

Table 7 - Imaginary Frequencies, Dipole Moments, Total Energies and Relative Energies of the Symmetric 2nd Order TS of Lycopene Model B Isomers

Conformer	Imaginary Frequencies (cm^{-1})		Dipole	Energy (Hartree)	ΔEnergy ($kcal \cdot mol^{-1}$)
Trans	115.5i	51.0i	1.1343	-424.6036305	5.4827
5-*Cis*	77.1i	19.6i	1.0753	-424.6055073	4.305

6.2 Molecular Structure of full-Lycopene

6.2.1 Molecular configurations

The relative energies, which measure thermodynamic stabilities of lycopene isomers, are summarized in **Table 8** and are depicted in **Figure 7**. Four categories for *cis*-isomers were recognized earlier, which are summarized in **Table 1**.

The computed relative stabilities of the four categories of the *cis*-isomers, are listed below :

> *Type A'* involves the 5-*cis* isomer. This is the only *cis*-isomer which is slightly more stable (within –0.5 kcal•mol^{-1}) than the all-*trans* form.
> *Type A* involves the 9-*cis* and 13-*cis* isomers. These *cis* isomers are slightly less stable (within 1.0 kcal•mol^{-1}) than the all-*trans* form.
> *Type B* involves the 15-*cis* isomer, which is only about 3 kcal•mol^{-1} less stable than the all-*trans* form.
> *Type C* involves the 7- and 11-*cis* isomers. These *cis*-isomers are about 6 kcal/mol higher on the energy scale than the all-*trans* form.

Note that the *cis*-isomers of lycopene in *Types A'* and *A* and the *trans* lycopene have similar energies, since we are dealing with triply substituted double bonds as shown in **Table2**.

Type A structures (see **Figure 1** and **Table 4**) are only slightly higher on the energy scale (see **Figure 6**) than the all-*trans* isomer. *Type A'* is very similar to *Type A*, except that the hydrogens on the 1,4 positions (denoted as carbon 4 and 7) are not eclipsed but staggered. This is illustrated in **Table 8** and **Figure 6**. For *Type B*, there is only one example- the 15-*cis* isomer. The 1,4 interaction involves the *cis* double bond which has only two alkyl substituents as shown in **Table 8**.

TABLES

Table 8 – Computed Total Energy and Relative Energy Values of Various Isomers of Lycopene, at HF/3-21G level of theory

Isomer	Energy (Hartree)	Rel. Energy (kcal mol^{-1})
All-*trans*	-1538.5731249	0.000
5-Cis	**-1538.5737548**	**-0.395**
7-Cis	-1538.5636899	5.921
9-Cis	-1538.5722460	0.552
11-Cis	-1538.5634789	6.053
13-Cis	-1538.5721338	0.622
15-Cis	-1538.5693098	2.394

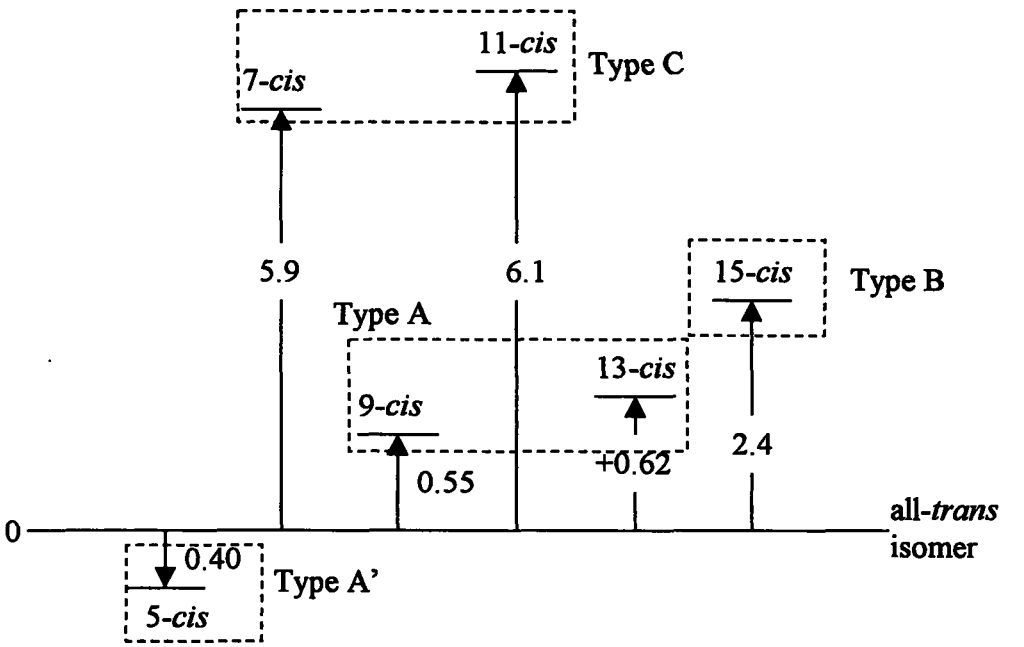

Figure 6 A schematic illustration of the relative energies (kcal•mol^{-1}) of the various *cis*-isomers of lycopene studied relative to the all-*trans* form

Type C has the two least stable structures, the 7-*cis* and 11-*cis* isomers. In accordance with **Figure 6,** the relative energies measuring stabilities are therefore as follows in **Scheme 11**.

In view of the foregoing, one only may wonder if the thermodynamic stability of the lycopene isomers, as well as the kinetic stability of the isomerization transition states, will predetermine the relative concentrations of these isomers in tissues and plasma.

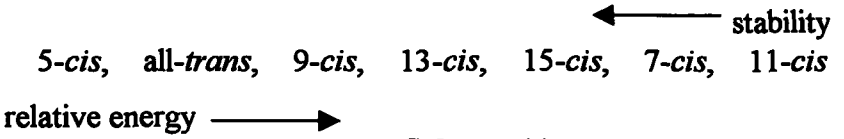

Scheme 11

Recent experimental finding[20] suggests that indeed the above thermodynamic stability dominates in the mixture and is made up primarily of the 5-*cis*, 9-*cis* and 13-*cis* isomers in addition to the all-*trans* form.

6.2.2 Molecular conformations

When a planar moiety is rotated about a tetrahedral carbon, it may be either eclipsed with a tetrahedral bond or perpendicular to that bond. This has been revealed by the study on ethyl benzene[18] and illustrated earlier in **Scheme 5**.

When dealing with the isomers lycopene, in most cases the olefinic moiety seems to favour a compromising position, having χ_2 and χ_4 in the range of 90°-107°. Thus, it is either roughly perpendicular to the C^3-C^4 bond or near to a position of eclipsing with one of the two C-H bonds of the CH_2 moieties of C^3 and C^4. The optimized values of the torsional angles are summarized in **Table 9**.

Figure 7 shows the optimized structures of lycopene in the all-*trans* as well as in the 5-*cis* isomeric form. The results (see **Figure 7** and **Table 9**) clearly indicate that while the conjugated double bonded segment of lycopene from C^5 to $C^{5'}$ is planar or nearly planar, the two terminal positions of the molecule (from C^1 to C^5 as well as from $C^{1'}$ to $C^{5'}$) are rotated out of plane.

Table 9 - Optimized torsional angles and selected orbital energies for various isomers of lycopene, calculated at RHF/3-21G level of theory.

Parameter[a]	Dihedral	all-*trans*	5-*cis*	7-*cis*	9-*cis*	11-*cis*	13-*cis*	15-*cis*
χ_2	D5	-106.596	103.040	-106.539	-106.605	-106.440	-106.409	-106.393
χ_3	D6	-176.424	176.517	-176.567	-176.479	-176.430	-176.524	-176.473
χ_4	D7	-100.364	90.063	-100.548	-100.368	-100.340	-100.393	-100.459
χ_2'	D31	106.368	106.440	106.515	106.460	106.394	106.474	106.475
χ_3'	D30	176.452	176.460	176.480	176.460	176.4637	176.504	176.456
χ_4'	D29	100.377	100.406	100.468	100.415	100.448	100.415	100.421
ϕ	D#	N/A	1.388	-5.854	-0.016	5.945	-0.0005	0.016
HOMO	-	-0.23712	-0.23320	-0.23387	-0.23347	-0.23508	-0.23422	-0.23459
LUMO	-	+0.06964	+0.05102	+0.05144	+0.05255	+0.06867	+0.05331	+0.05284
Δ	-	0.30676	0.28422	0.28531	0.28602	0.30375	0.28753	0.28743

a) χ Denotes the dihedral angle value for the C-C bonds, from the outsides inwards ($\therefore \chi_2$ corresponds to the first single bond, closest to the terminal end of the molecule). ϕ corresponds to the value of the dihedral angle about which the isomerisation has occured, for each particular *cis*-isomer. Thus, ϕ measures deviation from coplanarity of the *cis* double bond. HOMO is Highest Occupied MO energy, measuring the ionisation energy (IE) in terms of Koopman's theorem. LUMO is Lowest Unoccupied MO energy and Δ is the difference LUMO-HOMO in Hartree atomic units.

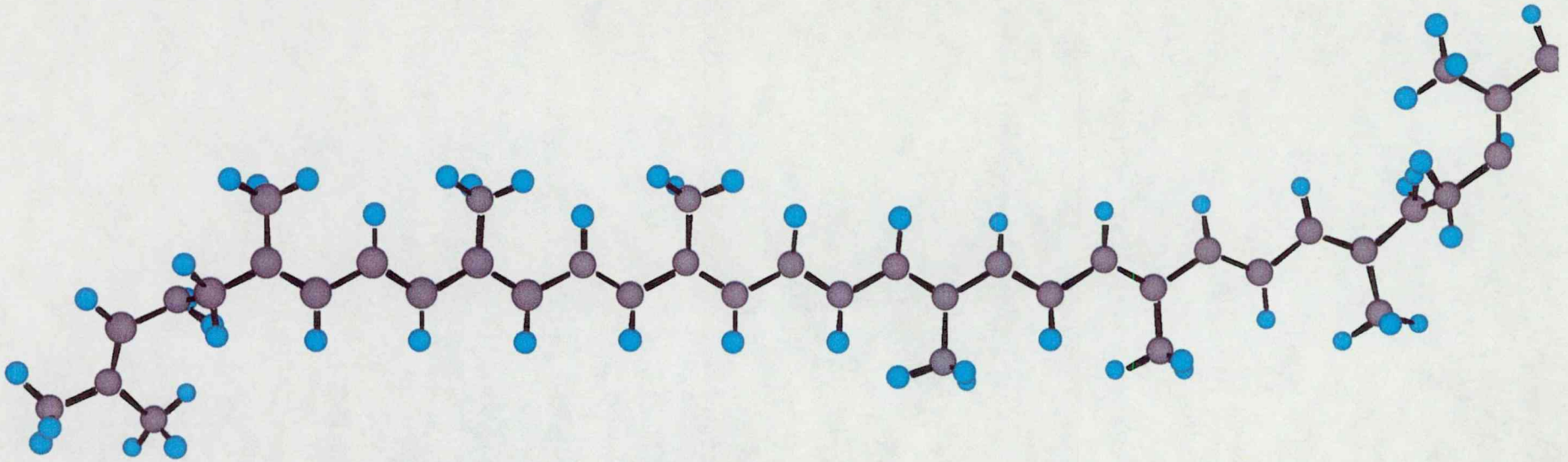

SIDE VIEW

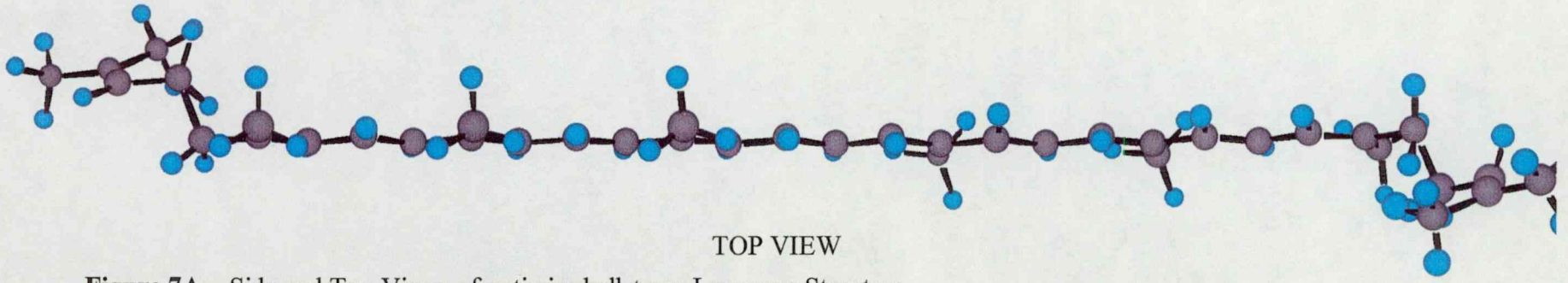

TOP VIEW

Figure 7A – Side and Top Views of optimised all-*trans* Lycopene Structure

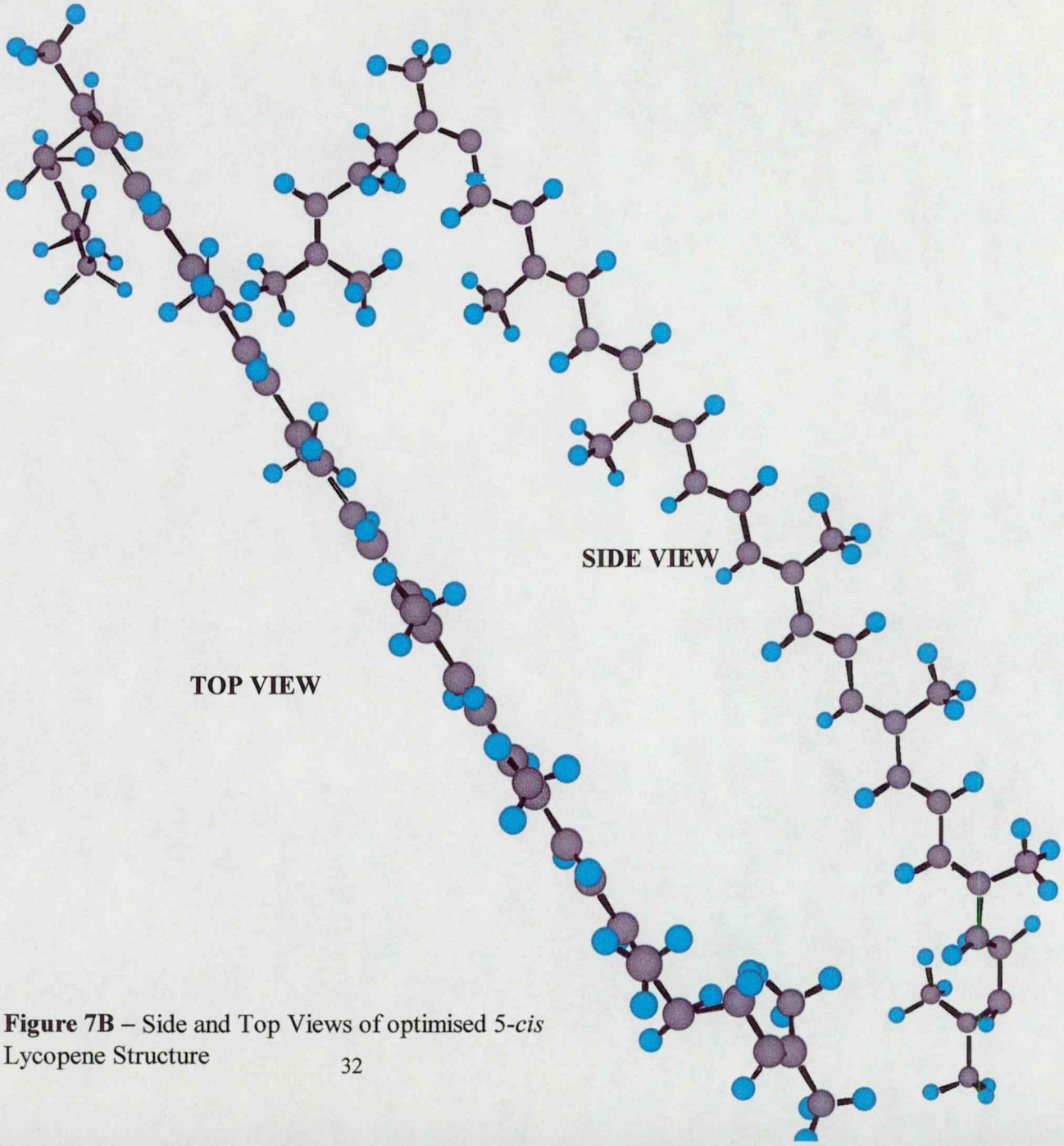

Figure 7B – Side and Top Views of optimised 5-*cis* Lycopene Structure

6.2.3 Deviation from Coplanarity

Sometimes the reactivity of an unsaturated compound is related to its not completely planar forms. This is particularly true for *cis*- double bonds. Deviation from coplanarity of the *cis*-isomers is within about 6° at the HF/3-21G level of theory as shown by the data in **Table 9** by the entry ϕ. The deviation from coplanarity ($\Delta\phi$) at the corresponding double bonds in the all *trans*-form is considerably smaller (within 1.5°) as shown by the data given in **Table 10**. Such non-planarity implies a weakening of the π-bond, which in turn is related to reactivity. Such an enhanced reactivity is certainly related to *trans-/cis* isomerization. However, it is not clear at this time if such structural differences may also imply enhanced radical scavenging ability.

Table 10- Torsional angles for the *trans*-peptide bonds in the all-*trans* lycopene, computed at RHF/3-21G level of theory.

Bond	Dihedral (ϕ)	ϕ	$\Delta\phi$ [a]
C^{1}-C^{2}	D4	178.955	1.045
C^{5}-C^{6}	D8	178.645	1.355
C^{7}-C^{8}	D10	179.943	1.057
C^{9}-C^{10}	D12	-179.999	-0.001
C^{11}-C^{12}	D14	179.999	0.001
C^{13}-C^{14}	D16	179.998	0.002
C^{15}-$C^{15'}$	D18	180.000	0.000
$C^{14'}$-$C^{13'}$	D20	179.997	0.003
$C^{2'}$-$C^{11'}$	D22	180.000	0.000
$C^{10'}$-$C^{9'}$	D24	180.000	0.000
$C^{8'}$-$C^{7'}$	D26	179.060	0.940
$C^{6'}$-$C^{5'}$	D28	-178.623	-0.377
$C^{2'}$-$C^{1'}$	D32	-178.925	-0.075

a) Deviation from coplanarity measured as follows:
$\Delta\phi = 180° - \phi$ (for $\phi > 0$)
$\Delta\phi = -180° - \phi$ (for $\phi < 0$)

6.3 Putative Isomerization Reaction Mechanism of Lycopene Model C

6.3.1 Structures and stabilities, along the isomerization mechanism pathway of lycopene Model C

The *trans-cis* isomerization mechanism (**Figure 8**) of **Model C**, as well as the conformational torsional angles and relative energies of its intermediates have been examined in detail. The geometries energies and stabilities of all species involved are presented in **Table 11**.

Results obtained here for the neutral compounds are expected to follow the sequence of energy and stability of the full lycopene. The observed order of stability is clearly in agreement with earlier results obtained in the case of full lycopene :

5-*cis* > all-*trans* > 7-*cis* **(9)**

For the cationic intermediates, the order of stability is different :

all-*trans* > 5-*cis* > 7-*cis* **(10)**

For the three cationic intermediates (i.e. for the all-*trans*, the 5-*cis* and 7-*cis* cations of **Model C**), the

$$E = E(\chi_3) \quad (11)$$

PECs are shown in **Figure 9**. It is interesting to note that the cationic intermediates show the presence of two minima; one in the vicinity of 120° and the other one in the vicinity of -120° (i.e. 240°). The higher energy minimum corresponds to an arrangement when both trigonal plananr moieties are eclipsing the same hydrogen of the adjacent CH_2, while in the lower minima, each of the two trigonal planar carbons is eclipsing different hydrogens of the adjacent CH_2.

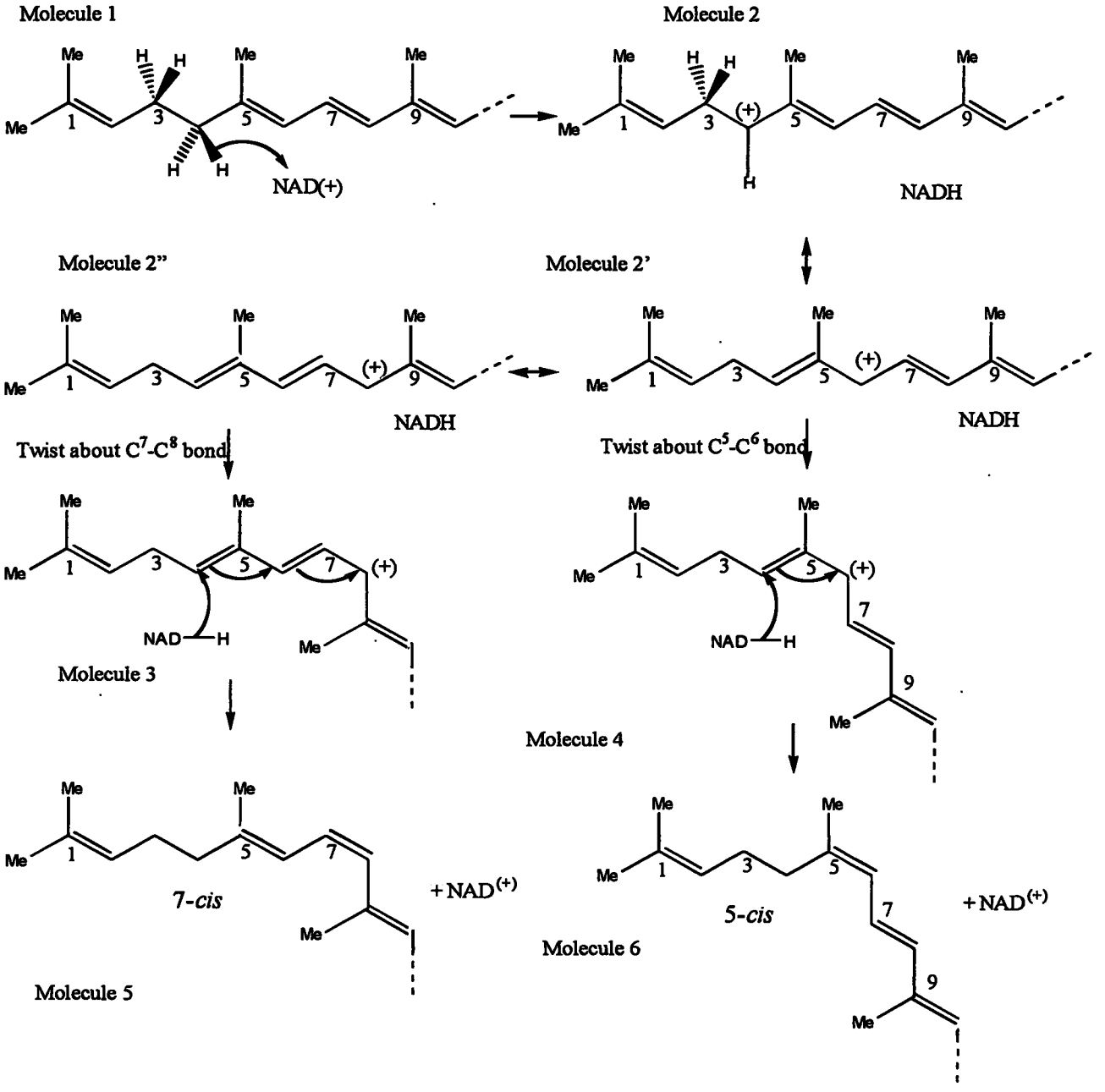

Figure 8 Putative mechanism for lycopene isomerization

Table 11 - Torsional angles, total and relative energies for the reactant, intermediates and products of lycopene Model C isomerization

Isomer	Charge	χ_1	χ_2[a]	χ_3[a]	χ_4[a]	χ_5[b]	χ_6	χ_7[b]	χ_8	χ_9	χ_{10}[c]	χ_{11}[c]	χ_{12}[c]	Energy (Hartree)	ΔE (kcal mol^{-1})
All-*trans*	0	-178.919	106.090	176.414	100.211	-178.62	-179.773	-179.942	179.977	179.996	179.853	175.917	-179.006	-539.8927057	0.000000
5-*cis*	0	-178.918	103.058	176.448	90.186	*1.362*	-178.146	179.905	-179.779	-179.990	179.197	175.871	-179.943	-539.8933291	-0.391190
7-*cis*	0	181.069	106.427	176.351	99.600	181.633	182.021	*0.772*	181.454	180.274	179.991	173.943	177.585	-539.8833670	5.860127
All-*trans*	+1	179.161	97.958	99.284	-177.597	-178.327	179.673	-179.958	179.979	-179.971	-179.741	-2.318	179.980	-539.0853808	0.000000
5-*cis*	+1	179.030	97.370	100.087	-177.362	*2.951*	-179.406	180.000	-0.003	-0.001	-179.933	-178.288	179.894	-539.0790704	3.959839
7-*cis*	+1	179.102	98.443	98.994	-177.642	-178.235	179.713	*0.098*	-179.968	179.995	-179.667	-2.413	179.875	-539.0750170	6.503388

a) **Conformational torsional angles, in bold**
b) ***Cis*-isomeric torsional angles, in *italics***
c) **Methyl Rotations**

Table 12 - Variation of carbon-carbon bond lengths along the isomerization pathway of lycopene Model C

Molecule	Charge	R(Me-C_1)	R(C_1-C_2)	R(C_2-C_3)	R(C_3-C_4)	R(C_4-C_5)	R(C_5-C_6)	R(C_6-C_7)	R(C_7-C_8)	R(C_8-C_9)	R(C_9-C_{10})
All-*trans*	0	1.517	**1.321**	1.510	1.556	1.518	**1.328**	*1.462*	**1.328**	*1.472*	**1.325**
5-*cis*	0	1.517	**1.321**	1.510	1.556	1.517	**1.328**	*1.463*	**1.328**	*1.472*	**1.325**
7-*cis*	0	1.517	**1.321**	1.510	1.556	1.518	**1.329**	*1.463*	**1.332**	*1.478*	**1.326**
All-*trans*	1	1.516	**1.322**	1.529	1.495	**1.359**	*1.410*	*1.393*	*1.364*	**1.335**	1.516
5-*cis*	1	1.516	**1.323**	1.531	1.495	**1.358**	*1.412*	*1.399*	*1.362*	**1.334**	1.515
7-*cis*	1	1.516	**1.322**	1.529	1.495	**1.360**	*1.412*	*1.394*	*1.368*	**1.337**	1.516

Footnote
Conjugated single bonds in *Italics*
Double bonds in **Bold**
R[C-C] in ethane = 1.542 in butadiene = 1.467
R[C=C] in ethylene = 1.315 in butadiene = 1.320

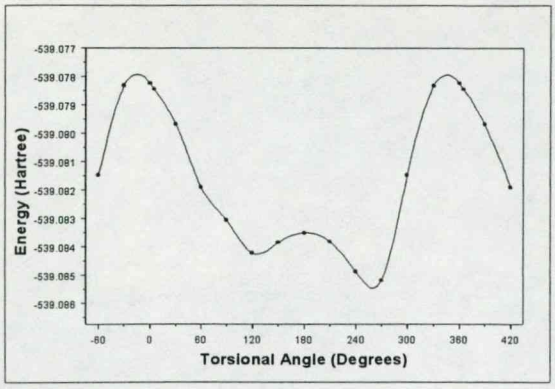

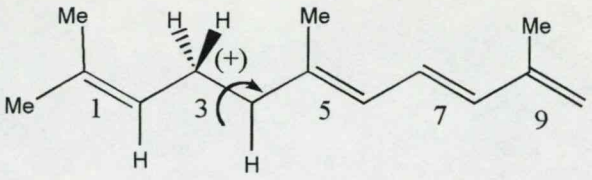

all trans

D (C2 -C3-C4-C5)

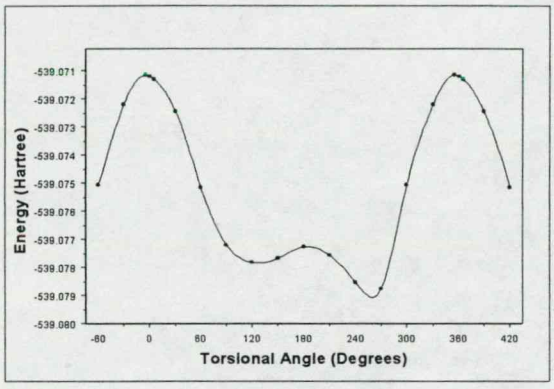

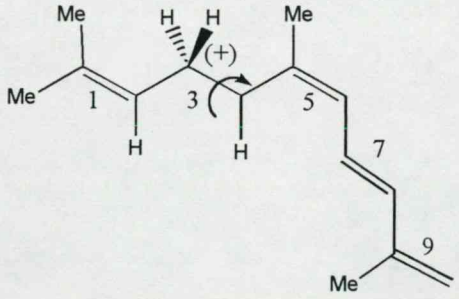

5- cis

D (C2 -C3-C4-C5)

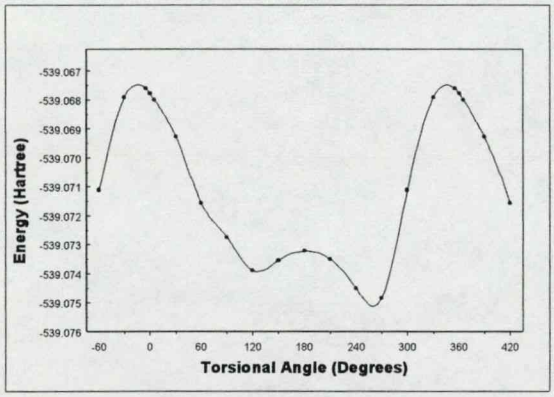

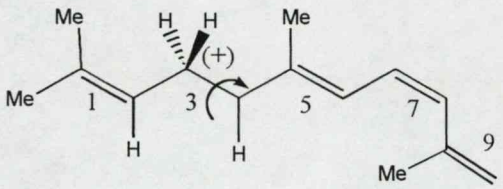

7-cis

D (C2 -C3-C4-C5)

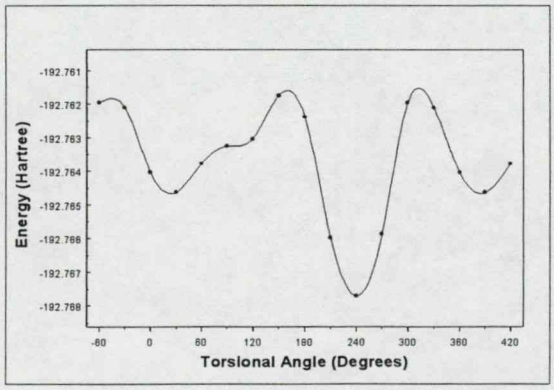

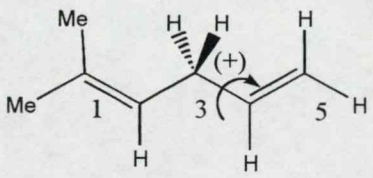

1,4-pentadiene

D (C2 -C3-C4-C5)

Figure 9 Torsional potentials for the three cationic intermediates of lycopene **ModelC** isomerization. **Top :** All-*trans* **Middle :** 5-*cis* **Bottom :** 7-*cis*

6.3.2 Bond Length Interpretations

One of the structural features of the isomerization process is the changing carbon-carbon bond length. During the reaction, a double bond may change to a single bond and *vice versa*. Key bond lengths at various stages of isomerization are summarised in **Table 12**. The C-C single and C=C double bond lengths, obtained at this level of theory, are given for the sake of comparison, in the footnote of **Table 12**.

Three types of CC bond lengths were identified :

Double bond (approximately : 1.32Å)

Conjugated single bond (approximately : 1.47Å)

Genuine single bond (approximately : 1.54Å)

On the basis of that a conjugated stabilization pattern has emerged, which is shown in **Figure 10**. The results (**Table 12** and **Figure 10**) roughly coincide with the expected changes, but they are somewhat different from conventional resonance hybrid representation (c.f. Structures 2, 2' and 2" in **Figure 9**).

all-trans

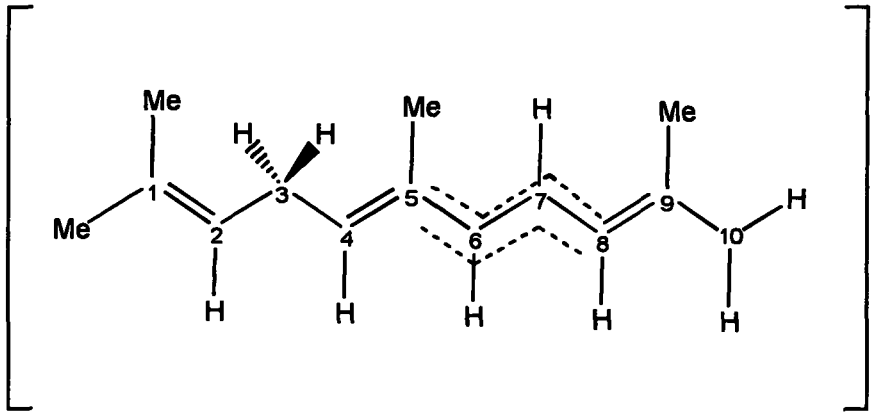

7-cis

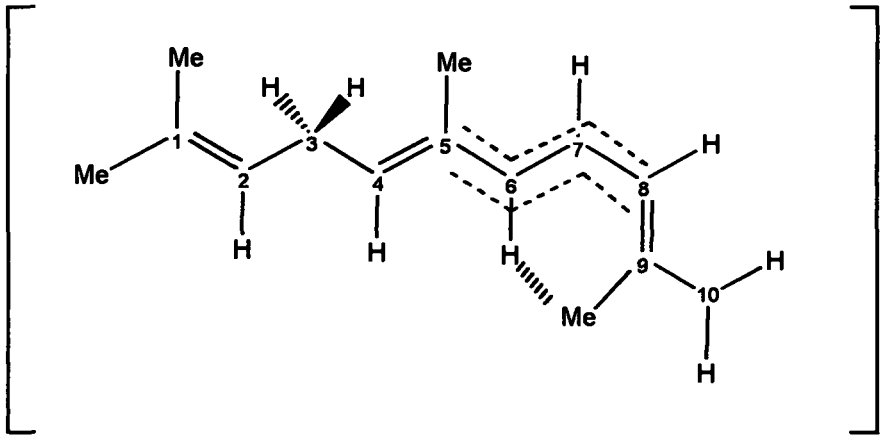

5-cis

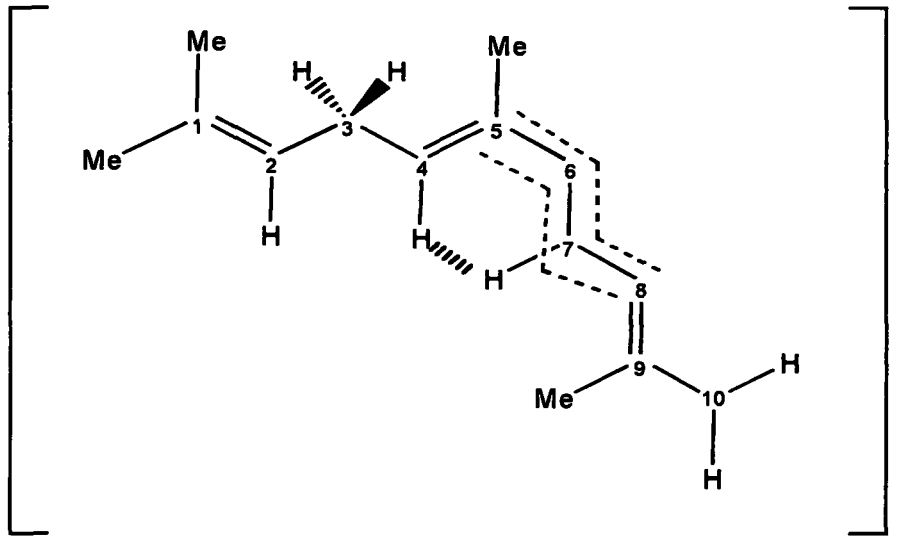

Figure 10 Delocalized scheme for π-electrons of three cationic isomers of **Model C**. **Top :** all *trans*- **Center :** 7-*cis*-isomer **Bottom :** 5-*cis*-isomer. The structures are drawn to show the key torsional angle (C_2-C_3-C_4-C_5) involved at 180° **Figure 10**

6.3.3 *Energetics of isomerization mechanism*

The rotational potential energy curves associated with the isomerization processes

All-*trans* cation → 5-*cis* cation

All-*trans* cation → 7-*cis* cation

are shown in **Figure 11**. The barriers to interconversions are different for the two processes. The two PECs clearly indicate that the isomerization to the 5-*cis* cation is kinetically more favourable than that to the 7-*cis* cation; however, the cations have to be formed in the first place. Hydride transfer to $NAD^{(+)}$ may lead to the formation of allylic cations.

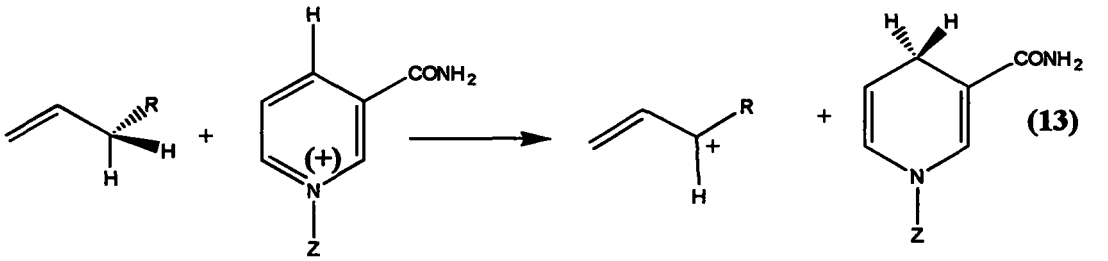

(13)

The relative ease of hydride [$H:^{(-)}$] removal is measured by the hydride affinity of the molecular system. Hydride affinity values, as computed at the RHF/3-21G level of theory, are summarized in **Table 13**. These data suggest that the easiest removal of an allylic hydride is from the all-*trans* isomer and the most difficult to remove, is from the 5-*cis* isomer. These results are illustrated graphically by **Figure 12**, in the form which preserves the mechanistic considerations given in **Figure 8**.

As far as the thermodynamics of the reaction are concerned, a great deal depends on the hydride affinity of the hydride acceptor. This is clearly shown in **Figure 13** where a weak hydride acceptor [$Li^{(+)}$] is compared to a strong hydride acceptor [$H_3C^{(+)}$], as summarized in **Table 13**. The overall reaction may be endothermic for a weak hydride acceptor [$Li^{(+)}$], or exothermic for a strong hydride acceptor [$H_3C^{(+)}$], as shown in **Figure14**.

No attempt is made here to study $NAD^{(+)}$ because it is believed that the hydride affinity of $NAD^{(+)}$ is not just the hydride affinity of the pyridinium ring. It is quite likely modified by the carbohydrate attached, as well as by the remaider of the $NAD^{(+)}$ molecule.

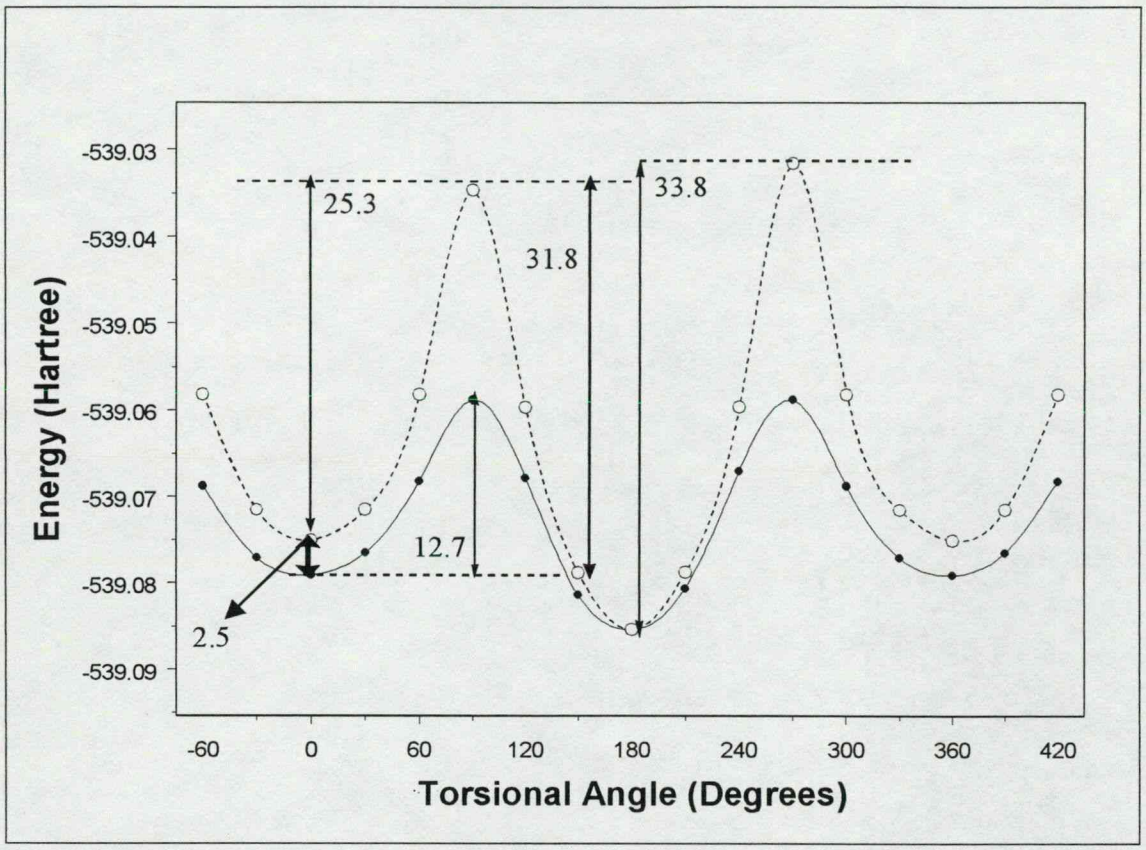

Figure 11 Torsional potentials for the two isomerization processes **Solid Line :** All-*trans* → 5-*cis* **Broken Line :** All-*trans* → 7-*cis*

Table 13 - Energy components[a] for hydride affinities of selected compounds

Molecular System	Total Energy (Hartree)		Hydride Affinity (kcal•mol^{-1})
	Cation	Neutral	
Weak Hydride Acceptor	-7.1870945 $Li^{(+)}$	-7.9298426 Li-H	214.814
Strong Hydride Acceptor	-39.0091291 $H_3C^{(+)}$	-39.9768768 H_3C-H	356.003
All-*trans* **Model C**	-539.0853808	-539.8927057	255.336
5-*cis* **Model C**	-539.0790704	-539.8933291	259.687
7-*cis* **Model C**	-539.0750170	-539.8833670	255.980

[a] **$E[H^{(-)}] = -0.4004207$ Hartree**

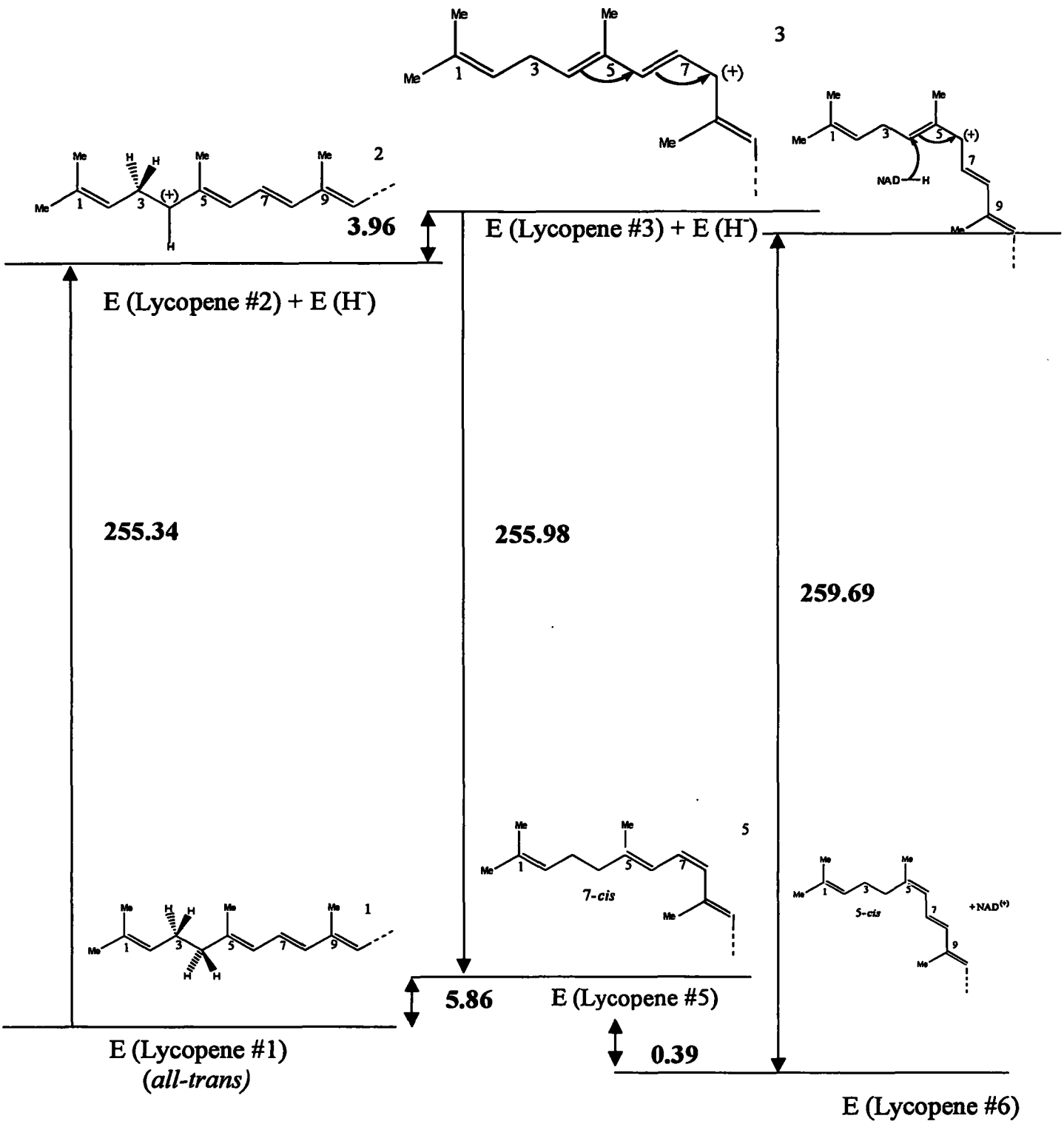

Figure 12 Energy level diagram (kcal•mol^{-1}) for trans-cis isomerization mechanism of the truncated lycopene model

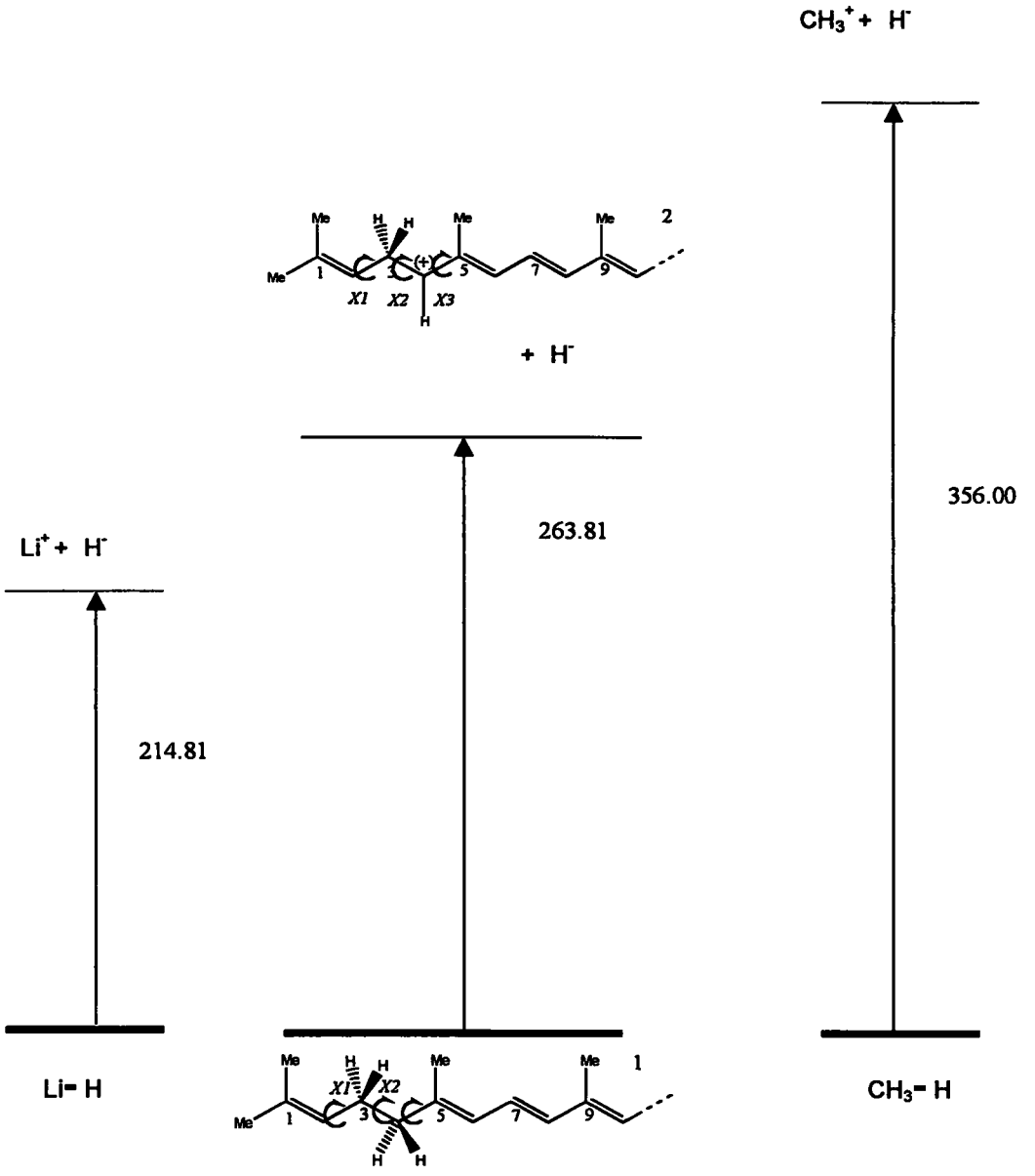

Figure 13 Side-by-side comparison of hydride affinities (kcal•mol^{-1}) for several small cationic systems

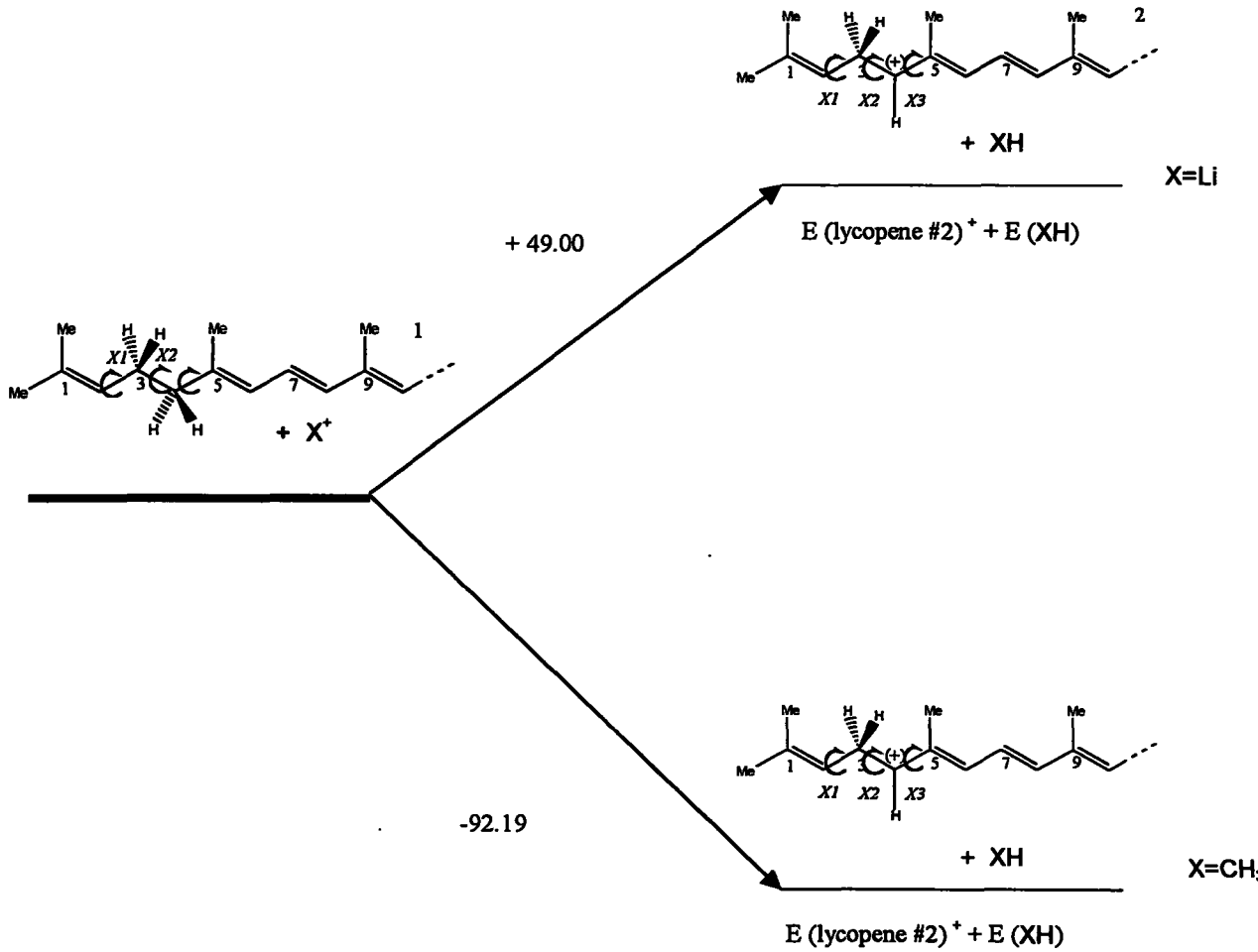

Note: Bolded lines = reactants

Figure 14 Energy level diagram (kcal•mol^{-1}) for hydride ion transfer from neutral all-*trans* lycopene **Model C** to selected cationic species

7. POSSIBLE BIOLOGICAL CONSEQUENCES

Epidemiological studies have supported the hypothesis that consumption of heat processed tomatoes, such as in the Mediterranean diet, may reduce the risk of coronary heart disease by preventing the oxidation of the low-density lipoprotein [5,6]. Giovannucci *et al.* have also suggested that only the intake of processed tomato products was related to reduced risk of prostate cancer, probably because of their high *cis* isomer content of lycopene [21]. The observation that high concentration of *cis* isomers are present in human serum and prostate tissue also suggests, that *cis* isomers might be biologically more active than the all-*trans* isomer.

Note that in human plasma, lycopene is an isomeric mixture containing at least 60% of the total lycopene as a mixture of *cis*-isomer (see **Table 14**). The mixture of the *cis*-lycopenes probably contains 5-*cis*, 9-*cis* and 13-*cis* isomers[20].

Table 14- Amounts of lycopene in various substances and the percentages of *trans* and *cis* isomers present

	Total Lycopene[a]	**% *trans* (of total)**	**% *cis* (of total)**
Raw Tomato	233.58 ± 2.98 μM	89.70	10.30
Tomato juice	189.25 ± 1.12 μM	90.62	9.38
Heated Tomato Juice	178.08 μM	71.94	28.06
Human Serum	422.1 ± 22.9 nM	32.37	67.63
Rat Serum	36.41 ± 5.62 nM	37.74	62.26
Rat Prostate	316.66 ± 55.88 nM	33.38	66.62

a) consider the density of animal and plant tissues as 1, MW of lycopene as 536.85

8. CONCLUSIONS

In contrast to traditional expectation, according to which the *cis*-isomer is always less stable than the corresponding *trans*-isomer, the present study suggests at least the 5-*cis*-isomer is more stable than the all-*trans*-isomer. Such stability may be due to the favourable **Type A'** 1,4-interaction (**Scheme 4**). The conformational study revealed that the fully planar structure of lycopene **Model B** is a second-order saddle point. Such completely symmetric (i.e. planar) structure of the full-lycopene would be expected to become a fourth-order critical point on its PEHS, because there are two negative eignevalues at both ends (χ_2, χ_4 as well as $\chi_{2'}$, $\chi_{4'}$).

For the neutral compunds, the following order of stability is observed :

5-*cis* > all-*trans* > 9-*cis* > 13-*cis* > 15-*cis* > 7-*cis* > 11-*cis* **(14)**

According to the conformational study, the tail-ends of lycopene are not coplanar because the three torsional modes along the three carbon-carbon single bonds (=CH-CH_2-CH_2-CH_2), allows the considerable twisting. These allylic -CH_2 units may easily undergo hydride transfer, producing a cationic intermediate (=CH-CH_2-C^+H-CH=), which could more easily undergo *trans-cis* isomerization than the neutral lycopene. A putative mechanism is postulated for such isomerization.

9. REFERENCES

1. D. W. Laight, M. J. Carrier, E. E. Anggard, Cardiovasc Res 47 (2000) 457
2. A. Carr, B. Frei, Free Radic Biol Med. 28 (2000) 1806
3. S. Taddei, A. Virdis, L. Ghiadoni, G. Salvetti, A. Salvetti, J. Nephrol 13 (2000) 205
4. O. D. Saugstad, Acta Paediatr 89 (2000) 905
5. A. V. Rao;S. Agarwal. Nutr. Res. 19 (1999) 305-323
6. S. K Clinton. Nutr. Res. 56 (1998) 35-51
7. E. Giovannucci. J Natl Cancer Ins. 91 (1999) 317-331
8. R. Willstätter.; H. H. Escher. Z. Physiol. Chem. 64 (1910) 47-61
9. **(a)** P. Karrer; R. P. Widmer. Helv. Chim. Acta 11(1928) 751-752
   (b) P. Karrer; A. Helfenstein; R. P. Widmer. Helv. Chim. Acta 11(1928) 1201-1209
   (c) P. Karrer; W. E. Bachmann. Helv. Chim. Acta 12 (1929) 285-291
   (d) P. Karrer.; A. Helfenstein.; H. Wehrli.; A. P. Wettstein. Helv. Chim. Acta. 13 (1930)1084-1099.
10. L. Zechmeister; A. L. LeRosen; W. A. Schroeder; A. Polgar; L. Pauling. J. Am. Chem. Soc. 65 (1943) 1940-1955
11. L. Zechmeister; P. Tuzson. Nature. 141 (1938) 249-250
12. A. Polgar; L. Zechmeister. J. Am. Chem. Soc. 64 (1942) 1856-1861
13. L. Zechmeister; A. Polgar. J. Am. Chem. Soc. 65 (1943) 1522-1528
14. L. Zechmeister; R. B. Escue. J. Am. Chem. Soc. 66 (1944) 322-330
15. L. Pauling. Fortschr. Chem. organ. Naturstoffe. 3 (1939) 203-235
16. **(a)** C. Sterling. Acta Crystallogr. 17 (1964) 1224-1228
    (b) M. O. Senge, H. Hope; K. M. Smith. Z.Naturforsch.,Teil C. 47 (1992) 474-480
17. Gaussian 98, Revision A.9, M. J. Frisch, G. W. Trucks, H. B. Schlegel, G. E. Scuseria, M. A. Robb, J. R. Cheeseman, V. G. Zakrzewski, J. A. Montgomery, Jr., R. E. Stratmann, J. C. Burant, S. Dapprich, J. M. Millam, A. D. Daniels, K. N. Kudin, M. C. Strain, O. Farkas, J. Tomasi, V. Barone, M. Cossi, R. Cammi, B. Mennucci, C. Pomelli, C. Adamo, S. Clifford, J. Ochterski, G. A. Petersson, P. Y. Ayala, Q. Cui, K. Morokuma, D. K. Malick, A. D. Rabuck, K. Raghavachari, J. B. Foresman, J. Cioslowski, J. V. Ortiz, A. G. Baboul, B. B. Stefanov, G. Liu, A. Liashenko, P.

Piskorz, I. Komaromi, R. Gomperts, R. L. Martin, D. J. Fox, T. Keith, M. A. Al-Laham, C. Y. Peng, A. Nanayakkara, M. Challacombe, P. M. W. Gill, B. Johnson, W. Chen, M. W. Wong, J. L. Andres, C. Gonzalez, M. Head-Gordon, E. S. Replogle, and J. A. Pople, Gaussian, Inc., Pittsburgh PA, 1998.

18. Ö. Farkas, S. J. Salpietro; P. Császár; I. G. Csizmadia. J. Mol. Struct (THEOCHEM) 367 (1996) 25-31

19. J. G. Angyan, R. Daudel, A. Kucsman and I. G. Csizmadia. Chem. Phys. Letters 136 (1987) 1-8

20. R. Re, P. D. Fraser, H. Long, P. M. Bramley and C. Rice-Evans. Biochemical and Biophysical Research Communications 281 (2001) 576-581

21. E. Giovannucci, A. Aschevio, E. B. Rimm, M. J. Stampfer, G. H. Coldiz, W. C. Willett. J. Nat. Cancer Inst. 87 (1995) 1767-1776

10. APPENDICES

Appendix A

Small basis set calculations usually lead to uneven charge distribution. The more electronegative atoms accumulate higher electron density than their share and the less electronegative atoms lose electron density unduly. This means an excessive charge build up resulting in more attraction or more repulsion than the appropriate. A larger basis set compensates for this uneven distribution of electron density. However, within the Hartree-Fock formalism it still does not allow for proper electron correlation. For that, a post-Hartree-Fock method is needed which conveniently may be achieved at the level of Density Functional Theory such as B3LYP.

In this Appendix, the full-lycopene calculations are presented at three levels of theory so that a comparison of the three set of results may be made.

The full lycopene geometries and energies are summarized in **Tables A1-A3**. The relative energies are compared on the top portion of **Figure 1A**. The relative energy values compared at higher levels of theory, when plotted against ΔE[HF/3-21G] are scattered in the vicinity of the 45° line indicating that while the correlation is not perfect the trend is the same for all three levels of theory applied.

Table A1 – Computed total energy and Relative Energy Values of Various Isomers of Lycopene, computed at the RHF/3-21G level of theory

Isomer	Energy (Hartree)	Rel. Energy (kcal mol^{-1})
All-*trans*	-1538.5731249	0.000
5-Cis	**-1538.5737548**	**-0.395**
7-Cis	-1538.5636899	5.921
9-Cis	-1538.5722460	0.552
11-Cis	-1538.5634789	6.053
13-Cis	-1538.5721338	0.622
15-Cis	-1538.5693098	2.394

Table A2 – Computed total energy and Relative Energy Values of Various Isomers of Lycopene, computed at the RHF/6-31G(d) level of theory

Isomer	Energy (Hartree)	Rel. Energy (kcal mol^{-1})
All-*trans*	-1547.17308770	0.000
5-Cis	**-1547.17330879**[a]	**-0.139**
7-Cis	-1547.16378778[a]	5.836
9-Cis	-1547.17212827	0.602
11-Cis	-1547.16361049[a]	5.947
13-Cis	-1547.17201904[a]	0.671
15-Cis	-1547.16877570[a]	2.706

[a] Convergency on energy is estimated within 0.000015 hartrees or ~0.01 kcal•mol^{-1}

Table A3 – Computed total energy and Relative Energy Values of Various Isomers of Lycopene, computed at theB3LYP/6-31G(d) level of theory

Isomer	Energy (Hartree)	Rel. Energy (kcal mol^{-1})
All-*trans*	-1557.87137336	0.000
5-Cis	**-1557.87142948**	**-0.035**
7-Cis	-1557.86297700	5.269
9-Cis	-1557.86988472	0.934
11-Cis	-1557.86365446	4.844[b]
13-Cis	-1557.86970859	1.045[b]
15-Cis	-1557.86618002	3.259

[a] Convergency on energy is estimated within 0.000015 hartrees or ~0.01 kcal•mol^{-1}

[b] Only partial convergency is achieved. Energies are therefore higher than expected, perhaps by 0.5 kcal•mol^{-1}

Appendix B

Small basis set calculations usually lead to uneven charge distribution. The more electronegative atoms accumulate higher electron density than their share and the less electronegative atoms lose electron density unduly. This means an excessive charge build up resulting in more attraction or more repulsion than the appropriate. A larger basis set compensates for this uneven distribution of electron density. However, within the Hartree-Fock formalism it still does not allow for proper electron correlation. For that, a post-Hartree-Fock method is needed which conveniently may be achieved at the level of Density Functional Theory, such as B3LYP.

For lycopene **Model C**, **Tables B1-B6** summarize the geometrical parameters as well as the total and relative energies. The relative energies are compared for the various isomers, in **Table B7**. The energies associated with the hydride abstractors and hydride donors are summarized in **Tables B8-B10**.

It may be noted that for the Lycopene **Model C** relative energies have monotonically declined, in the absolute sense. For example, in the case of the 5-*cis* isomer, there was a change from –0.391 through –0.289 to –0.076, all in kcal•mol^{-1}. Similarly, for the 7-*cis* isomer, the variation involved a change from +0.5860 through +5.534 to + 4.658, on going from RHF/3-21G to RHF/6-31G(d) all way the to B3LYP/6-31G(d), levels of theory. For the cations, the change was not monotomic, but instead all changes occurred within a 1 kcal•mol^{-1} range.

It might be added that not only the energetic changes are small, but the geometrical changes are also minor, when the level of theory is improved.

All in all, the conclusion may be drawn from the tabulated data that no fundamental change in the thermodynamic trend may be observed when the level of theory is improved. Thus, the previously published RHF/3-21G results represented a fairly accurate description of the chemistry studied.

Table B1 - Torsional angles, total and relative energies for the reactant, intermediates and products of lycopene Model C isomerization, computed at the RHF/3-21G level of theory

Isomer	Charge	χ_1	χ_2[a]	χ_3[a]	χ_4[a]	χ_5[b]	χ_6	χ_7[b]	χ_8	χ_9	χ_{10}[c]	χ_{11}[c]	χ_{12}[c]	Energy (Hartree)	ΔE (kcal mol^{-1})
All-*trans*	0	-178.919	**106.090**	**176.414**	**100.211**	-178.62	-179.773	-179.942	179.977	179.996	179.853	175.917	-179.006	-539.8927057	0.000
5-*cis*	0	-178.918	**103.058**	**176.448**	**90.186**	*1.362*	-178.146	179.905	-179.779	-179.990	179.197	175.871	-179.943	-539.8933291	-0.391
7-*cis*	0	181.069	**106.427**	**176.351**	**99.600**	181.633	182.021	*0.772*	181.454	180.274	179.991	173.943	177.585	-539.8833670	5.860
All-*trans*	+1	179.161	**97.958**	**99.284**	-177.597	-178.327	179.673	-179.958	179.979	-179.971	-179.741	-2.318	179.980	-539.0853808	0.000
5-*cis*	+1	179.030	**97.370**	**100.087**	-177.362	*2.951*	-179.406	180.000	-0.003	-0.001	-179.933	-178.288	179.894	-539.0790704	3.960
7-*cis*	+1	179.102	**98.443**	**98.994**	-177.642	-178.235	179.713	*0.098*	-179.968	179.995	-179.667	-2.413	179.875	-539.0750170	6.503

Table B2 - Torsional angles, total and relative energies for the reactant, intermediates and products of lycopene Model C isomerization, computed at the RHF/6-31G(d) level of theory

Isomer	Charge	χ_1	χ_2[a]	χ_3[a]	χ_4[a]	χ_5[b]	χ_6	χ_7[b]	χ_8	χ_9	χ_{10}[c]	χ_{11}[c]	χ_{12}[c]	Energy (Hartree)	ΔE (kcal mol^{-1})
All-*trans*	0	180.225	**115.099**	**178.759**	**112.615**	180.876	180.315	-179.843	179.955	179.973	178.673	194.307	180.053	-542.9051897	0.000
5-*cis*	0	180.267	**114.498**	**175.273**	**92.765**	*0.532*	180.656	-180.062	180.112	180.028	178.806	176.056	179.924	-542.9055506	-0.226
7-*cis*	0	180.196	**115.553**	**178.421**	**113.855**	181.713	182.721	*0.847*	180.481	180.230	178.744	202.218	178.300	-542.8963676	5.536
All-*trans*	+1	178.982	**104.068**	**106.454**	181.325	181.396	179.759	-179.988	180.006	180.006	179.889	-2.743	179.987	-542.1021042	0.000
5-*cis*	+1	178.844	**104.452**	**108.808**	181.465	*2.699*	180.373	-179.898	179.999	179.991	179.547	182.792	179.957	-542.0949436	4.493
7-*cis*	+1	178.944	**104.124**	**105.858**	181.247	181.603	179.781	*0.084*	179.962	179.993	179.358	-2.996	179.838	-542.0916754	6.544

Table B3 - Torsional angles, total and relative energies for the reactant, intermediates and products of lycopene Model C isomerization, computed at the B3LYP/6-31G(d) level of theory

Isomer	Charge	χ_1	χ_2[a]	χ_3[a]	χ_4[a]	χ_5[b]	χ_6	χ_7[b]	χ_8	χ_9	χ_{10}[c]	χ_{11}[c]	χ_{12}[c]	Energy (Hartree)	ΔE (kcal mol^{-1})
All-*trans*	0	180.105	**117.820**	**178.653**	**109.877**	180.796	180.031	-179.901	179.934	180.009	179.041	183.673	179.919	-546.692548	0.000
5-*cis*	0	180.719	**116.900**	**175.489**	**97.043**	*0.855*	180.624	-179.974	179.920	180.059	178.955	177.045	179.919	-546.6926685	-0.076
7-*cis*	0	180.844	**115.956**	**177.589**	**108.434**	181.005	180.840	*0.294*	179.911	180.176	179.825	181.775	179.661	-546.6851250	4.658
All-*trans*	+1	178.616	**96.715**	**95.829**	182.387	183.780	179.306	-180.209	180.014	180.032	182.846	-3.043	180.257	-545.8487503	0.000
5-*cis*	+1	178.343	**93.891**	**96.430**	183.000	*6.122*	181.008	-179.642	180.126	179.909	182.300	177.629	179.641	-545.8428732	3.688
7-*cis*	+1	178.737	**95.128**	**95.278**	182.422	183.717	179.402	*-0.400*	179.796	179.976	181.869	-2.386	180.382	-545.8402749	5.318

a) Conformational torsional angles, in bold
b) *Cis*-isomeric torsional angles, in *italics*
c) Methyl Rotations

Table B4 - Variation of carbon-carbon bond lengths along the isomerization pathway of lycopene Model C, computed at RHF/3-21G

Molecule	Charge	R(Me-C_1)	R(C_1-C_2)	R(C_2-C_3)	R(C_3-C_4)	R(C_4-C_5)	R(C_5-C_6)	R(C_6-C_7)	R(C_7-C_8)	R(C_8-C_9)	R(C_9-C_{10})
All-*trans*	0	1.517	**1.321**	1.510	1.556	1.518	**1.328**	*1.462*	**1.328**	*1.472*	**1.325**
5-*cis*	0	1.517	**1.321**	1.510	1.556	1.517	**1.328**	*1.463*	**1.328**	*1.472*	**1.325**
7-*cis*	0	1.517	**1.321**	1.510	1.556	1.518	**1.329**	*1.463*	**1.332**	*1.478*	**1.326**
All-*trans*	1	1.516	**1.322**	1.529	1.495	**1.359**	*1.410*	*1.393*	*1.364*	*1.442*	**1.335**
5-*cis*	1	1.516	**1.323**	1.531	1.495	**1.358**	*1.412*	*1.399*	*1.362*	*1.443*	**1.334**
7-*cis*	1	1.516	**1.322**	1.529	1.495	**1.360**	*1.412*	*1.394*	*1.368*	*1.449*	**1.337**

Table B5 - Variation of carbon-carbon bond lengths along the isomerization pathway of lycopene Model C, computed at RHF/6-31G(d)

Molecule	Charge	R(Me-C_1)	R(C_1-C_2)	R(C_2-C_3)	R(C_3-C_4)	R(C_4-C_5)	R(C_5-C_6)	R(C_6-C_7)	R(C_7-C_8)	R(C_8-C_9)	R(C_9-C_{10})
All-*trans*	0	1.511	**1.325**	1.507	1.542	1.514	**1.331**	*1.465*	**1.331**	*1.473*	**1.327**
5-*cis*	0	1.511	**1.325**	1.507	1.543	1.515	**1.331**	*1.465*	**1.331**	*1.473*	**1.327**
7-*cis*	0	1.511	**1.325**	1.507	1.542	1.514	**1.333**	*1.466*	**1.335**	*1.479*	**1.328**
All-*trans*	1	1.510	**1.327**	1.519	1.495	**1.361**	*1.416*	*1.396*	*1.369*	*1.445*	**1.337**
5-*cis*	1	1.509	**1.327**	1.519	1.495	**1.360**	*1.420*	*1.400*	*1.366*	*1.447*	**1.336**
7-*cis*	1	1.509	**1.327**	1.519	1.495	**1.362**	*1.417*	*1.398*	*1.373*	*1.451*	**1.339**

Table B6 - Variation of carbon-carbon bond lengths along the isomerization pathway of lycopene Model C, computed at B3LYP/6-31G(d)

Molecule	Charge	R(Me-C_1)	R(C_1-C_2)	R(C_2-C_3)	R(C_3-C_4)	R(C_4-C_5)	R(C_5-C_6)	R(C_6-C_7)	R(C_7-C_8)	R(C_8-C_9)	R(C_9-C_{10})
All-*trans*	0	1.511	**1.342**	1.505	1.553	1.513	**1.353**	*1.449*	**1.354**	*1.460*	**1.347**
5-*cis*	0	1.511	**1.342**	1.505	1.553	1.513	**1.353**	*1.449*	**1.354**	*1.460*	**1.347**
7-*cis*	0	1.511	**1.342**	1.505	1.553	1.514	**1.356**	*1.451*	**1.359**	*1.465*	**1.349**
All-*trans*	1	1.507	**1.350**	1.526	1.486	**1.386**	*1.413*	*1.404*	*1.381*	*1.439*	**1.358**
5-*cis*	1	1.506	**1.352**	1.525	1.485	**1.386**	*1.415*	*1.406*	*1.380*	*1.440*	**1.357**
7-*cis*	1	1.507	**1.351**	1.525	1.486	**1.387**	*1.414*	*1.405*	*1.387*	*1.444*	**1.359**

Footnote : Conjugated single bonds in *Italic* Double bonds in **Bold**

R[C-C] in ethane = 1.542 in butadiene = 1.467

R[C=C] in ethylene = 1.315 in butadiene = 1.320

Table B7 – Comparison of relative energies of neutral and cationic Lycopene Model B isomers

	Neutral			Cation		
Isomer	**RHF/3-21G**	**RHF/6-31G***	**B3LYP/ 6-31G(d)**	**RHF/3-21G**	**RHF/6-31G***	**B3LYP/ 6-31G(d)**
All-*trans*	0.000	0.000	0.000	0.000	0.000	0.000
5-*cis*	-0.391	-0.226	-0.076	3.960	4.493	3.688
7-*cis*	5.860	5.536	4.658	6.503	6.544	5.318

Table B8 - Energy components[a] for hydride affinities of selected compounds computed at the RHF/3-21G level of theory

Molecular System	Total Energy (Hartree)		Hydride Affinity ($kcal \cdot mol^{-1}$)
	Cation	Neutral	
Weak Hydride Acceptor	-7.1870945 $Li^{(+)}$	-7.9298426 Li-H	214.814
Strong Hydride Acceptor	-39.0091291 $H_3C^{(+)}$	-39.9768768 H_3C-H	356.003
All-*trans* **Model C**	-539.0853808	-539.8927057	255.336
5-*cis* **Model C**	-539.0790704	-539.8933291	259.687
7-*cis* **Model C**	-539.0750170	-539.8833670	255.980

[a] $E[H^{(-)}] = -0.4004207$ Hartree

Table B9 - Energy components[b] for hydride affinities of selected compounds computed at the RHF/6-31G(d) level of theory

Molecular System	Total Energy (Hartree)		Hydride Affinity ($kcal \cdot mol^{-1}$)
	Cation	Neutral	
Weak Hydride Acceptor	-7.2355365 $Li^{(+)}$	-7.9808683 Li-H	202.618
Strong Hydride Acceptor	-39.2306398 $H_3C^{(+)}$	-40.1951719 H_3C-H	340.167
All-*trans* **Model C**	-542.1021042	-542.9051897	238.858
5-*cis* **Model C**	-542.0949436	-542.9055506	243.577
7-*cis* **Model C**	-542.0916754	-542.8963676	239.866

[b] $E[H^{(-)}] = -0.422442$ Hartree

Table B10 - Energy components[c] for hydride affinities of selected compounds computed at the B3LYP/6-31G(d) level of theory

Molecular System	Total Energy (Hartree)		Hydride Affinity ($kcal \cdot mol^{-1}$)
	Cation	Neutral	
Weak Hydride Acceptor	-7.2845444 $Li^{(+)}$	-8.081922 Li-H	210.568
Strong Hydride Acceptor	-39.4803877 $H_3C^{(+)}$	-40.5183829 H_3C-H	361.558
All-*trans* **Model C**	-545.8487503	-546.6925480	239.697
5-*cis* **Model C**	-545.8428732	-546.6926685	243.460
7-*cis* **Model C**	-545.8402799	-546.6851250	240.354

[c] $E[H^{(-)}] = -0.4618167$ Hartree